Intermittency in nonlinear dynamics and singularities at complex times

Uriel Frisch
Division of Applied Sciences, Harvard University, Cambridge, Massachusetts 02138
*and Centre National de la Recherche Scientifique, Observatoire de Nice, BP 252, 06007 Nice-Cedex, France**

Rudolf Morf
Lyman Laboratory of Physics, Harvard University, Cambridge, Massachusetts 02138
*and Laboratories RCA, Badenerstrasse 569, 8048 Zurich, Switzerland**

(Received 30 June 1980)

High-pass filtering of turbulent velocity signals is known to produce intermittent bursts. This is, as shown, a general property of dynamical systems governed by nonlinear equations with band-limited random forces or intrinsic stochasticity. It is shown that singularities for complex times determine the very-high-frequency behavior of the solution and show up in the high-pass filtered signal as bursts centered at the real part of the singularity and with overall amplitude decreasing exponentially with the imaginary part. Near a singularity, nonlinear interactions, however weak they may be on the real axis, acquire unbounded strength. Investigations of singularities by nonperturbative methods is thus essential for quantitative analysis of high-frequency or high-wave-number properties. In contrast to results based on two-point closures, the high-frequency dissipation-range spectrum is actually not universal with respect to the low-frequency forcing. Unlimited intermittency is demonstrated, i.e., the flatness of the high-pass filtered solution grows indefinitely with filter frequency. This gives strong support to a conjecture of Kraichnan [Phys. Fluids **10**, 2080 (1967)] about intermittency in the dissipation range of turbulent flows. The analysis is carried out in great detail for the nonlinear Langevin equation $m\dot{v} = -\gamma v - v^3 + f(t)$. Lorenz's three mode system and Burgers's model are also discussed. Conjectures are made about Navier-Stokes turbulence which can be checked experimentally and numerically.

I. INTRODUCTION

A. Small-scale intermittency in turbulent flows

It is known since the work of Batchelor and Townsend[1] that the small scales of high-Reynolds number turbulence are intermittent; in other words, the high-frequency or high-wave-number turbulent activity comes in bursts separated by relatively long quiescent periods. Figure 1 shows a typical intermittent signal obtained by high-pass filtering the output of a hot wire measuring velocity fluctuations in a turbulent flow.[2]

Univariate distributions of unfiltered turbulent signals are known to be nearly Gaussian.[3] A quantitative measure of the deviation from Gaussian statistics is given by the flatness F, ratio of the fourth-order moment to the square of the second-order moment. For a centered Gaussian $F = 3$; for an intermittent signal F can be roughly thought of as the ratio of quiescent to active time.

An overall measure of the intermittency of a given flow is provided by the flatness of the longitudinal velocity derivatives $\partial^n u/\partial t^n$; this flatness increases monotonically both with Reynolds number and order of derivative.[1,4] The data, which have a considerable scatter, are consistent with a power-law dependence on Reynolds number (see Fig. 13 of Ref. 4). Band-pass filtering rather than differentiation of the velocity signal, before measuring the flatness, gives information on the scale dependence of intermittency. We note that (i) the temporal structure of signals measured at a given point reflects mostly the spatial structure of the velocity field in the frame of the mean velocity ("Taylor hypothesis"); (ii) spectral analysis of high-Reynolds number flows reveals that there is a range of frequencies (scales) over which the dynamics of the flow are dominated by the inertial terms in the equation of motion; this "inertial range" extends up to a frequency ω_D consistent with Kolmogorov's[5] prediction: $\omega_D \sim \overline{U}(\epsilon/\nu^3)^{1/4}$, where $\overline{U}$ is the mean velocity, ϵ the energy dissipation per unit mass, and ν the kinematic viscosity. Beyond ω_D, in the "dissipation range", viscous dissipation becomes important. The data of Kuo and Corrsin (Fig. 16 of Ref. 4) show that intermittency increases with midband frequency throughout the inertial range and the beginning of the dissipation range, until signal-to- (nonturbulent) noise ratio deteriorates. This happens at about twice the Kolmogorov frequency. The direct analysis of the spatial structure made possible by numerical simulations also reveals intermittency of small scales.[6-8] Extrapolated to infinite Reynolds number, experimental and numerical data suggest indefinite growth of the flatness with midband frequency.

Starting with Landau's[9] observation pointing out a possible inconsistency between the Kolmogorov 1941 theory[5] and dissipation fluctuations (see also

FIG. 1. Intermittent velocity signal obtained by Gagne. The plot shows high-pass filtered output of a hot-wire probe measuring the velocity in grid-generated turbulent flow.

Sec. 25.1 of Ref. 10), there has been a considerable amount of work on intermittency which it is not our purpose to review here (see, e.g., Refs. 10–13). Existing theoretical work deals mostly with inertial-range intermittency and uses generally heuristic, not systematic, methods. Dissipation-range intermittency and dissipation-range dynamics, one of the main concerns of this paper, have not received much attention. This may be in part because of lack of reliable data, since under usual experimental conditions measurements in the dissipation range are strongly limited by probe size and signal-to-noise ratio problems.

The first qualitative analysis of dissipation-range intermittency was presented in a paper of Kraichnan[14] which we shall discuss in detail in Sec. I B. In this discussion we shall assume that the reader is familiar with some of the usual ideas and concepts of homogeneous turbulence. This is not a prerequisite for understanding the remainder of the paper. Indeed, we shall show that, what is known in turbulence as "dissipation-range intermittency," is also present in a large class of nonlinear systems not restricted to fluid-dynamical situations. Some readers may therefore wish to go directly to Sec. I C, which introduces a model much simpler than the Navier-Stokes equation, and to Sec. I D which contains the outline of the paper and gives the main theoretical ideas.

B. Discussion of Kraichnan's theory of dissipation-range intermittency

Kraichnan[14] was led to the following two conjectures.

(i) Turbulent flows have "unlimited intermittency" in the dissipation range, i.e., the flatness of the band-filtered velocity grows indefinitely with midband wave number.

(ii) Such intermittency is also present at very low Reynolds numbers.

The turbulent flows considered by Kraichnan satisfy the Navier-Stokes equation with a random driving force depending on space and time,

$$\partial_t \vec{v} + \vec{v} \cdot \vec{\nabla}\vec{v} = -\nabla p + \nu \nabla^2 \vec{v} + \vec{f}, \qquad \vec{\nabla} \cdot \vec{v} = 0. \tag{1.1}$$

The force is assumed homogeneous, isotropic, stationary, and so presumably, is the solution of the Navier-Stokes equation (after relaxation of transients). Note that, due to dissipation, a nonzero stationary state requires some energy input. In actual flows this is achieved by a variety of mechanisms (boundary conditions, buoyancy forces, prescribed shears, ...). The random force achieves the same goal, while allowing us to take advantage of the invariance of the Navier-Stokes equation under space and time translations and rotations.[15] A traditional justification of the

random force model is based on the *Universality assumption:* The properties of the very small scales of high-Reynolds number turbulence are independent of the driving mechanism (except for scaling factors).

A more cautious attitude is to use random forces to test universality: How sensitive are the (statistical) properties of small scales to the (statistical) properties of the random force? In order not to trivially spoil universality there should be no (or negligible) direct excitation of the small scales by the random force. The simplest is to take as Kraichnan[14] a *band-limited* force, i.e., whose spatial Fourier transform is restricted to wave numbers $k \leq k_0$. Spatial Fourier components of the stationary (henceforth understood to mean "statistically stationary") solution with wave numbers $k > k_0$ are then excited only by nonlinear interactions, and high wave numbers require repeated interactions.

In this setting, we first discuss Kraichnan's second conjecture, assuming that the flow is driven at very low Reynolds numbers. Wave numbers less than k_0 are then well approximated by ignoring the nonlinear terms. Beyond k_0 perturbation theory to some finite order (increasing with wave number) should be adequate. High wave numbers are then represented by high-order *functional* powers of the force. The effect of *ordinary* power raising of a random function is well understood: It makes the result increasingly intermittent because it emphasizes the largest excursions in the function. This is illustrated in Fig. 2 showing a Gaussian process and its fifth power. With functional powers the situation is not so clear because spatial and temporal integrations, mixing distant (and thereby weakly correlated) regions of the flow, tend to reduce intermittency. It is actually possible to construct a counterexample using, instead of the Navier-Stokes equation, the Markovian random coupling model which has the nonlinear term modified by random factors coupling N realizations of the flow.[16] In the limit $N \to \infty$, it is known that Gaussian statistics are obtained, so there is no intermittency. Of course, in this counterexample, the random coupling provides an extreme form of mixing.

We now turn to Kraichnan's first conjecture which is not restricted to low Reynolds numbers. Our presentation will differ somewhat from his. We need two assumptions.

(H1) The energy spectrum $E(k)$ at wave numbers far beyond k_0 has a universal shape.

$$E(k) \simeq A \tilde{E}(k/K_D), \quad k \gg k_0. \tag{1.2}$$

The function $\tilde{E}$ is universal with respect to the force but may depend on Reynolds number; A and K_D depend on the large-scale parameters of the flow (integral scale 1_0, mean energy input $\epsilon, \ldots$). According, for example, to the Kolmogorov 1941 theory,[5] $K_D \sim (\epsilon/\nu^3)^{1/4}$.

(H2) The function $\tilde{E}$ falls off faster than algebraically. This is equivalent to the existence of all spatial derivatives of the velocity in mean square.

At high Reynolds numbers, (H1) and (H2) seem well supported experimentally (see, for example, Fig. 75 in Ref. 10); however, existing data do not completely rule out algebraic fall-off with a large negative exponent as predicted, e.g., by Heisenberg's theory.[17]

Now, we use a two-step averaging argument inspired from Landau's[9] objection against the universality of the Kolmogorov constant (see also Ref. 10 Sec. 25.1; Ref. 1, Sec. 5; and Ref. 18, Sec. 5). Namely, we divide the flow into big cubic boxes of size $L \gg l_0$ and assume that, in each box, we can calculate the energy spectrum using the large-scale parameters obtained by space averaging over the box. Such parameters, e.g., the box-averaged energy input will still fluctuate slightly from box to box, and so will K_D. Owing to the faster than algebraic decrease, the amplitude of Fourier components with very high wave numbers will have arbitrary large fluctuations. Therefore, band-pass or high-pass[19] filtered velocities are expected to be very intermittent. Note that the above explanation of intermittency was briefly considered in Ref. 1 but not retained because algebraic decrease (assumed therein) would lead to an inconsistency with the data.

An interesting aspect of the above argument, not discussed by Kraichnan, is that it is self-destructive. Since the scaling parameters K_D and A vary randomly from box to box, the Grand averaged (i.e., averaged over all boxes) energy spectrum is

$$E(k) = \langle A(\epsilon, \ldots) \tilde{E}(k/K_D(\epsilon, \ldots)) \rangle, \tag{1.3}$$

averaged over ϵ and other large-scale parameters. Since $\tilde{E}$ decreases faster than algebraically, the averaging will generally change the functional form of the spectrum and make it dependent on the statistics of the random force and thus *nonuniversal*.

Finally, let us stress with Kraichnan a paradoxical aspect of dissipation-range intermittency. The Reynolds number based on local dissipation-range quantities is very small. Is this really compatible with intermittency which suggests strong nonlinear effects?

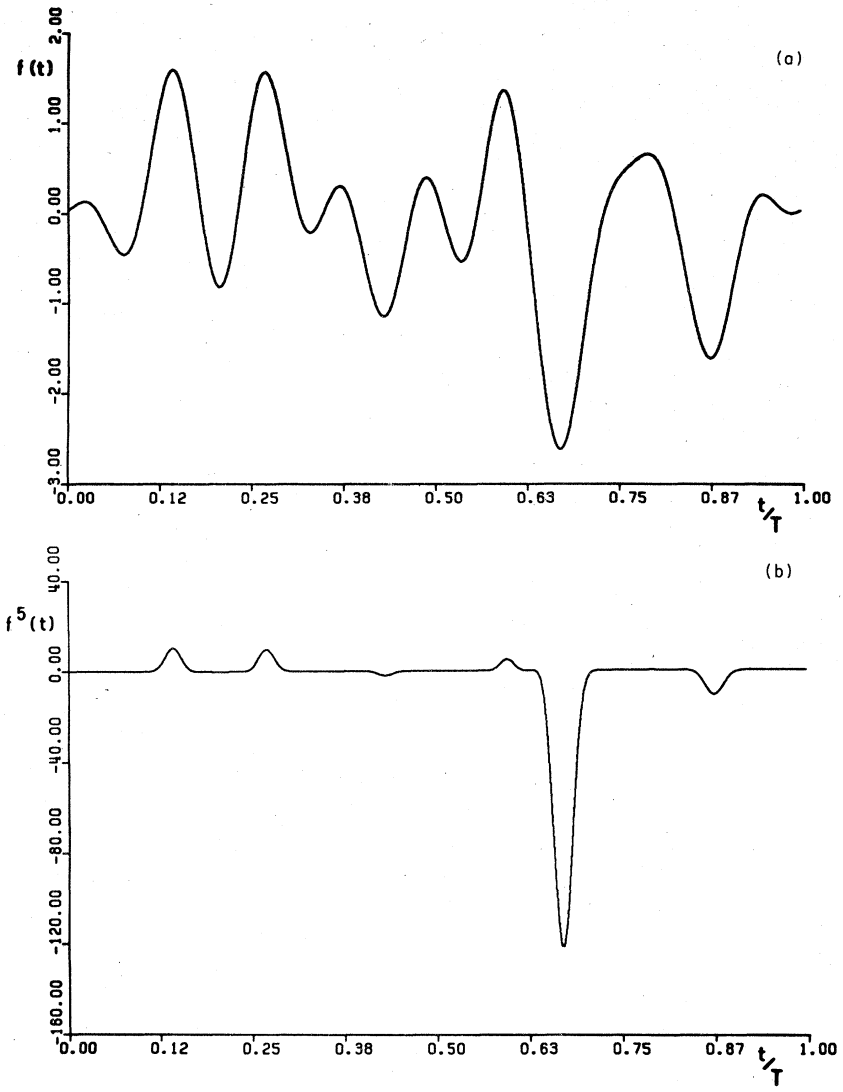

FIG. 2. (a) Gaussian process and (b) its fifth power.

C. Construction of a model

It is surprising how little use is made of the Navier-Stokes equation in Kraichnan's heuristic derivation of dissipation-range intermittency, discussed in Sec. I B. His argument should be applicable to any dynamical equation of motion such that (i) high wave numbers can be excited from band-limited input only through repeated nonlinear interactions, and (ii) there is a stationary solution with finite mean-square derivatives of all orders.

Once this is realized, it is natural to try to construct a model equation, much simpler than the Navier-Stokes equation, on which Kraichnan's conjectures can be tested. Spatial dependence is not needed, since we can apply the argument in the temporal domain. We are thus led to use a nonlinear ordinary differential equation (ODE) with band-limited random input as a model system. We choose the following very simple nonlinear Langevin (NLL) equation

$$m\dot{v} = -\gamma v - v^3 + f(t), \tag{1.4}$$

m and γ are positive parameters; the force $f(t)$ is a band-limited stationary random force with zero mean; the statistics of $f(t)$ are kept arbitrary to enable us to investigate universality questions.

We observe that a Riccati equation with quadratic nonlinearity (v^2 instead of v^3) would seem more in line with the Navier-Stokes equation. In some respects this is not so. First, if we assume that

the statistics of f and $-f$ are the same (this is true for Gaussian f), then in the cubic but not the quadratic case this property carries over to v, ensuring that $\langle v \rangle = 0$, as in homogeneous isotropic turbulence. Second, in the cubic equation the nonlinear term enhances the damping, thereby ensuring the existence of a solution for all times; for the Riccati equation this is not so, unless the force has a sufficiently small bound.

Nonlinear Langevin equations of similar forms are frequently used in connection with critical dynamics and various nonequilibrium phenomena.[20–23] Such studies are often concerned with the case $\gamma < 0$, leading to self-excitation. In all cases studied so far $f(t)$ is assumed to be Gaussian white noise or a related process; the equation can then be solved by Markov techniques. In such cases the high-frequency behavior is directly controlled by the force and intermittency is ruled out. With a band-limited force the high-frequency dynamics become nontrivial. However, the problem is no longer amenable to Markov techniques. Notice that the NLL equation corresponds to the electrical circuit shown in Fig. 3.

D. Outline of the paper

Section II is devoted to the nonlinear Langevin (NLL) equation. In Sec. II A we study the behavior for real times and present numerical evidence that the high-pass filtered solution is intermittent. In Sec. II B we show that the force, since it is band limited, can be continued to arbitrary complex times. The solution of the NLL equation is extended to complex times by a Weierstrass analytic continuation which is implemented numerically. Away from the real axis the solution has singularities, the nature of which is obtained analytically and the positions, at this point, numerically. In Sec. II C we show that the intermittent bursts in the high-pass filtered solution are related to singularities for complex times. This follows from standard results about Fourier transforms of analytic functions, connecting high-frequency asymptotics and singularities for complex times. In Sec. II D we calculate the statistical distribution of the "most relevant" singularities (close to the real axis). This is done by a singular perturbation method which takes advantage of the probabilistic nature of the problem. In Sec. II E we calculate the high-frequency behavior of the spectrum and the flatness; we prove that the solution has unlimited intermittency (flatness grows indefinitely with frequency) and is nonuniversal with respect to the force. The purely dissipative form of the nonlinearity does not allow energy-cascade-type arguments[5]; nevertheless we show in Sec. II F that at high Reynolds numbers the NLL model has an inertial range with power-law spectrum and with intermittency. In Sec. II G we make a comparison between our exact treatment of the NLL model and two-point closure, using the direct interaction approximation.[24]

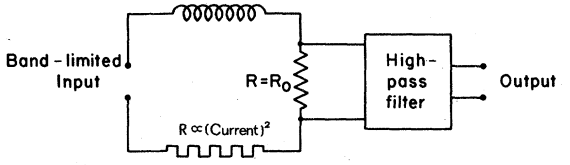

FIG. 3. Electrical analog circuit corresponding to the NLL equation (1.4).

In Sec. III we study intermittency in the Lorenz[25] model, an example of intrinsically stochastic system with no random force. In Sec. IV we study a partial differential equation, Burgers's[26] model, with spatial intermittency.

In Sec. V A we summarize and discuss the results obtained with the NLL model, many of which are not consistent with usual turbulence theories. In Sec. V B we discuss the shortcomings of field-theoretic methods when applied to the NLL model. In Sec. V C we show that intermittency is present in a large class of nonlinear systems and discuss conditions under which a quantitative analysis is possible. Section VI, devoted to Navier-Stokes turbulence, is speculative; we present conjectures about dissipation-range intermittency and suggest experimental and numerical tests.

II. THE NONLINEAR LANGEVIN (NLL) EQUATION

A. NLL equation in the real domain

Formulation

We are interested in the NLL equation

$$m\dot{v} = -\gamma v - v^3 + f(t), \quad m > 0, \quad \gamma > 0. \tag{2.1}$$

The force $f(t)$ is a real random function which satisfies the conditions listed below. A shorter list would be needed had we limited the analysis to Gaussian forces, thereby excluding the study of universality questions.

(F 1) The force $f(t)$ is stationary[27] in time. In addition, we assume either (P) $f(t)$ is periodic of period T, or (NP) $f(t)$ is nonperiodic and mixing (i.e., correlations tend to zero with increasing time separation).

(F 2) The force is symmetric: $f(t)$ and $-f(t)$ have identical statistics. Since the NLL equation is unchanged under simultaneous reversal of v and f, the stationary solution of (2.1), assuming

it exists, will also be symmetric. In particular, the expectation value of v (denoted by angular brackets) is zero,

$$\langle v(t)\rangle = 0 . \tag{2.2}$$

(F 3) The force is band limited with the following spectral representation

$$\text{(P)}\quad f(t) = \sum_{|\omega_n|\le B} \exp(-i\omega_n t)\hat{f}_n ;$$

$$\omega_n = \frac{2\pi n}{T} ; \quad n = 0, \pm 1, \pm 2, \ldots , \tag{2.3}$$

$$\text{(NP)}\quad f(t) = \int_{-B}^{+B} e^{-i\omega t}\hat{f}(\omega)\frac{d\omega}{2\pi} , \tag{2.4}$$

where B, the bandwidth, is a finite positive number, independent of the realization[28] chosen.

(F 4) The force and all its derivatives have finite moments of all order. $f(t)$ and $\dot{f}(t) = df(t)/dt$ are assumed, without loss of generality to have unit variance (by suitable rescaling).

(F 5) At the points where $f(t) = 0$, $\dot{f}(t)$ can take arbitrary large values with finite probability. This assumption will be needed in the singular perturbation calculation of Sec. II D.

An example of a force satisfying (F 1)–(F 5) is a Gaussian with a spectrum restricted to the interval $[-B, +B]$. (P) is satisfied with a discrete spectrum concentrated at frequencies ω_n. Given the Hermitian symmetry of $\hat{f}_n$, the total number of independent modes in the band is

$$N_M = 1 + [BT/(2\pi)], \tag{2.5}$$

where [ ] denotes the integral part. Condition (NP) is satisfied with a continuous spectrum.

Note that, from our assumptions, all derivatives of the force exist in mean square. Indeed, let us denote by $\hat{\Phi}(\omega)$ the energy spectrum of the force. Differentiating

$$\langle f(t)f(0)\rangle = \int_{-B}^{+B} e^{-i\omega t}\hat{\Phi}(\omega)\frac{d\omega}{2\pi} , \tag{2.6}$$

we obtain

$$\left\langle \left(\frac{d^s f(t)}{dt^s}\right)^2 \right\rangle = \int_{-B}^{+B} |\omega|^{2s}\hat{\Phi}(\omega)\frac{d\omega}{2\pi} \le B^{2s}\langle f^2\rangle = B^{2s} . \tag{2.7}$$

We want to solve the NLL equation subject to the following boundary conditions. In the nonperiodic case the velocity takes a prescribed real deterministic value at $t = t_0$. Then $t_0 \to -\infty$ so that $v(t)$ converges to the unique stationary solution of the NLL equation (as will be shown). Similarly, in the periodic case $v(t)$ is the unique periodic solution. The periodic case is of interest to us because numerical solutions of the NLL equations are, by necessity, restricted to a finite time interval $[0, T]$. We shall see in Sec. II C that the high-frequency behavior of the solution is governed by complex-time singularities of $v(t)$ which contribute exponentially decreasing terms to the Fourier transform $\hat{v}(\omega)$. A mismatch in the values at $t = 0$ and $t = T$ of $v(t)$ or any derivative produces the same effect in $\hat{v}(\omega)$ as a real-time singularity, namely an algebraically decreasing term which will then completely dominate the high-frequency region. Imposing periodicity suppresses algebraic terms. Windowing might constitute an alternative technique.[29]

One of the main goals of this paper is to calculate the high-frequency behavior of the energy spectrum

$$E(\omega) = \int_{-\infty}^{+\infty} e^{i\omega t}\langle v(t)v(0)\rangle\, dt , \tag{2.8}$$

and of the flatness

$$F(\Omega) = \langle v_\Omega^4(t)\rangle / \langle v_\Omega^2(t)\rangle^2 , \tag{2.9}$$

of the high-pass filtered velocity $v_\Omega(t)$, defined by

$$v_\Omega(t) = \int_{|\omega|\ge\Omega} e^{-i\omega t}\hat{v}(\omega)\frac{d\omega}{2\pi} , \tag{2.10}$$

in terms of the Fourier transform of the velocity

$$\hat{v}(\omega) = \int_{-\infty}^{+\infty} e^{i\omega t} v(t)\, dt . \tag{2.11}$$

In the periodic case, (2.10) and (2.11) become

$$v_\Omega(t) = \sum_{|\omega_n|\ge\Omega} \exp(-i\omega_n t)\hat{v}_n , \tag{2.12}$$

$$\hat{v}_n = \frac{1}{T}\int_0^T e^{i\omega t} v(t)\, dt . \tag{2.13}$$

Existence, uniqueness, and smoothness in the nonperiodic case

In the absence of cubic terms the Langevin equation with $v(t_0) = v_0$ has an explicit solution. Letting $t_0 \to -\infty$ for fixed v_0 one obtains

$$v(t) = \int_{-\infty}^{t} \exp\left(-\frac{\gamma}{m}(t - t_1)\right) f(t_1)\frac{dt_1}{m} . \tag{2.14}$$

Since the cubic term just provides additional damping, we can similarly transform the NLL equation into the integral equation

$$v(t) = \int_{-\infty}^{t} \exp\left(-\frac{1}{m}\int_{t_1}^{t} [\gamma + v^2(s)]\, ds\right) f(t_1)\frac{dt_1}{m} . \tag{2.15}$$

This equation can then be solved by iterations, starting from the linear solution; convergence is easily proved. To show uniqueness, we assume

the existence of two solutions $v_1(t)$ and $v_2(t)$. Subtracting, we obtain

$$\frac{d}{dt}(v_1 - v_2) = -(\gamma + v_1^2 + v_1 v_2 + v_2^2)(v_1 - v_2). \tag{2.16}$$

This, together with $v_1(t_0) = v_2(t_0)$, implies $v_1 = v_2$ for all times. Stationary of the solution (in the limit $t_0 \to -\infty$) follows from the stationarity of $f(t)$ and the translational invariance of the equation. It can also be shown that the solution is mixing; essentially, this follows from (i) the mixing assumption on $f(t)$ and (ii) the observation that, due to the exponential damping, the integral (2.15) has an effective range at most m/γ.

We now derive an upper bound for the variance of $v(t)$. From (2.15), we obtain

$$\langle v^2(t)\rangle \leq m^{-2} \int_{-\infty}^{t} \int_{-\infty}^{t} \exp\left(-\frac{\gamma}{m}(t - t_1 + t - t_1')\right) \times \langle |f(t_1)||f(t_1')|\rangle \, dt_1 \, dt_1'$$

$$\leq \frac{1}{\gamma^2}\langle f^2\rangle = \frac{1}{\gamma^2}. \tag{2.17}$$

Similarly, using (F 4), we see that all moments of $v(t)$ are finite.

Next, we estimate the mean-square derivative. Differentiating the NLL equation, we obtain, with $q = \dot{v}$,

$$m\dot{q} = -(\gamma + 3v^2)q + \dot{f}. \tag{2.18}$$

Hence

$$q(t) = \int_{-\infty}^{t} \exp\left(-\frac{1}{m}\int_{t_1}^{t} [\gamma + 3v^2(s)]\, ds\right) \dot{f}(t_1)\frac{dt_1}{m}. \tag{2.19}$$

Terminating the estimation as above, we obtain

$$\langle \dot{v}^2(t)\rangle \leq \frac{1}{\gamma^2}\langle \dot{f}^2\rangle = \frac{1}{\gamma^2}. \tag{2.20}$$

Similarly, all higher-order moments of $\dot{v}$ are finite. The result is extended to higher-order derivatives of $v(t)$ by induction, successively differentiating the NLL equation and using (F 4). From the finiteness of mean-square derivatives of all orders we infer that the spectrum $E(\omega)$ decreases faster than algebraically at high frequencies.

The periodic case

Most of the above results carry over to the periodic case. In addition, we have to prove existence and uniqueness of a periodic solution. Assume that $f(t)$ is periodic of period T. Consider the map

$$u \longmapsto \phi(u), \tag{2.21}$$

where $u = v(0)$ is an initial condition at $t = 0$ for the NLL equation and $\phi(u) = v(T)$. A fixed point of the map provides a periodic solution. We shall show that ϕ satisfies

$$|\phi(u_1) - \phi(u_2)| \leq e^{-\gamma T/m}|u_1 - u_2|. \tag{2.22}$$

This immediately implies convergence to a unique fixed point of the successive iterates of any u_0 and, thus, existence and uniqueness of the periodic solution. To prove (2.22) we notice that, for periodic $f(t)$, any solution (generally nonperiodic) satisfies

$$m\frac{d}{dt}[v(t+T) - v(t)] = -[\gamma + v^2(t+T) + v(t+T)v(t) + v^2(t)][v(t+T) - v(t)]. \tag{2.23}$$

Hence,

$$|v(2T) - v(T)| \leq e^{-\gamma T/m}|v(T) - v(0)|, \tag{2.24}$$

which is equivalent to (2.22).

Numerical evidence for intermittency

The NLL model is designed to test Kraichnan's[14] conjectures about dissipation-range intermittency. Solving it numerically with sufficient accuracy at very high frequencies requires great care, owing to the faster than algebraic decrease. Finite difference, spectral, and other standard numerical methods are very poorly suited for high-frequency studies in the presence of intermittency. We are led to use a Taylor expansion method combined with a Newton iteration to satisfy periodicity. The accuracy of the results reported in this paper is limited by roundoff only, except where Monte Carlo averaging is involved. All this is discussed in Appendix A.

Numerical evidence for intermittency is obtained by solving the NLL equation with $m = (0.3)^{1/2}$ and $\gamma = 0.1$; the force $f(t)$ is taken Gaussian, periodic with a flat spectrum ($B = \sqrt{3}$); the number of independent modes in the force is $N_M = 10$. The period is $T = 2\pi(30)^{1/2}$. Figure 4(a) shows one period of the force used. Figure 4(b) shows the unfiltered periodic solution and Figs. 4(c) and 4(d) show the corresponding high-pass filtered periodic solutions for two values of the filter frequency $\Omega/B = 3, \Omega/B = 10$. Note that the unfiltered solution resembles the force with minima and maxima at roughly the same positions [Figs. 4(a) and 4(b)]. The high-pass filtered signal appears in bursts. At $\Omega/B = 3$ [Fig. 4(c)], four small bursts begin to appear (at 0.1 T, 0.3 T, 0.6 T, and 0.9 T). As the filter frequency is increased the signal becomes increasingly intermittent. At

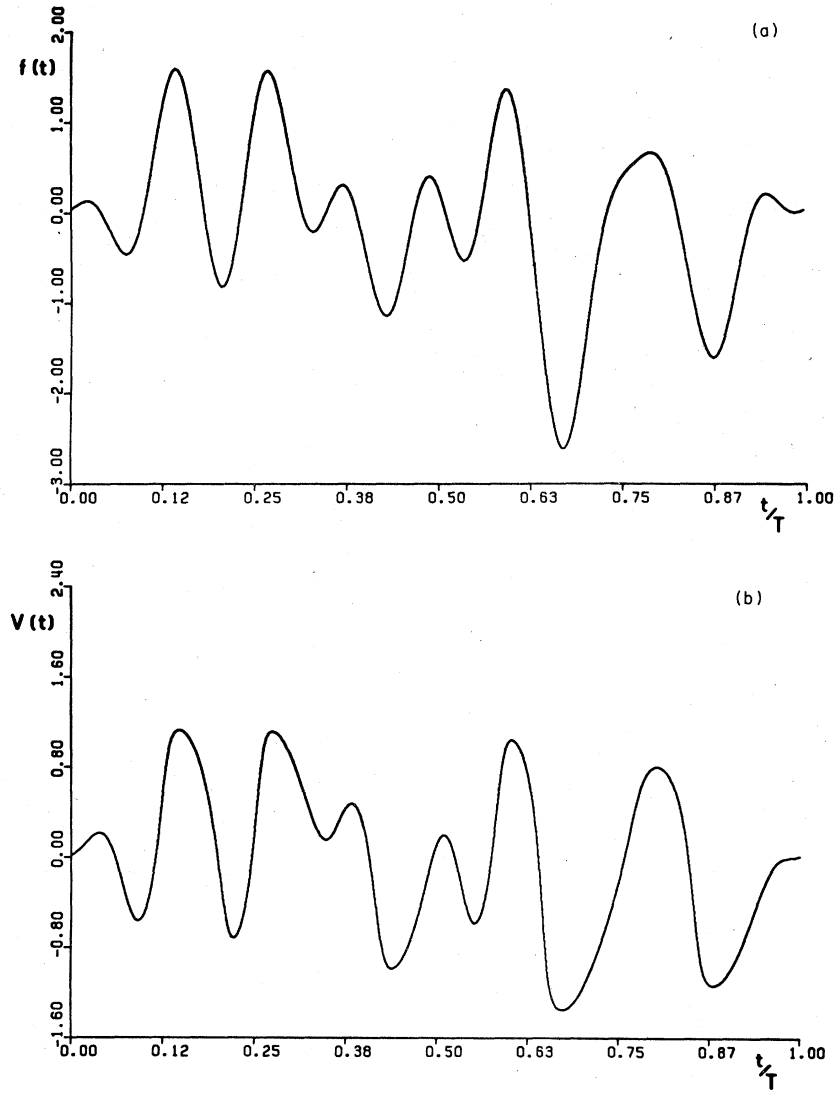

FIG. 4. Numerical evidence for intermittency. (a) shows one period of the force. (b) shows the unfiltered periodic solution. (c) and (d) show high-pass filtered solutions with filter frequencies corresponding to three and ten times the maximum excited mode in the force $f(t)$. Note that as the filter frequency is increased the signal shows an increasingly burstlike structure.

$\Omega/B = 10$ [Fig. 4(d)], the burst at $t = 0.6\ T$ dominates the signal with an amplitude roughly five times bigger than that of the second strongest burst centered at $t = 0.3\ T$. In Sec. II B and II C we shall see how the bursts in the high-pass filtered velocity can be understood by leaving the real-time domain.

B. NLL equation in the complex domain

The high-frequency behavior of the velocity is governed, as we shall see in Sec. II C, by the singularities of its analytic continuation to complex times. In this section, we show how the NLL equation can be extended into the complex-time domain. We begin with the analytic continuation of the force.

Analytic continuation of the force

The spectral representation of the force can be readily continued to complex times. Substituting $z = t + i\tau$ for t in (2.4), we obtain

$$f(z) = f(t + i\tau) = \int_{-B}^{+B} e^{-i\omega t} e^{\omega\tau} \hat{f}(\omega) \frac{d\omega}{2\pi} . \quad (2.25)$$

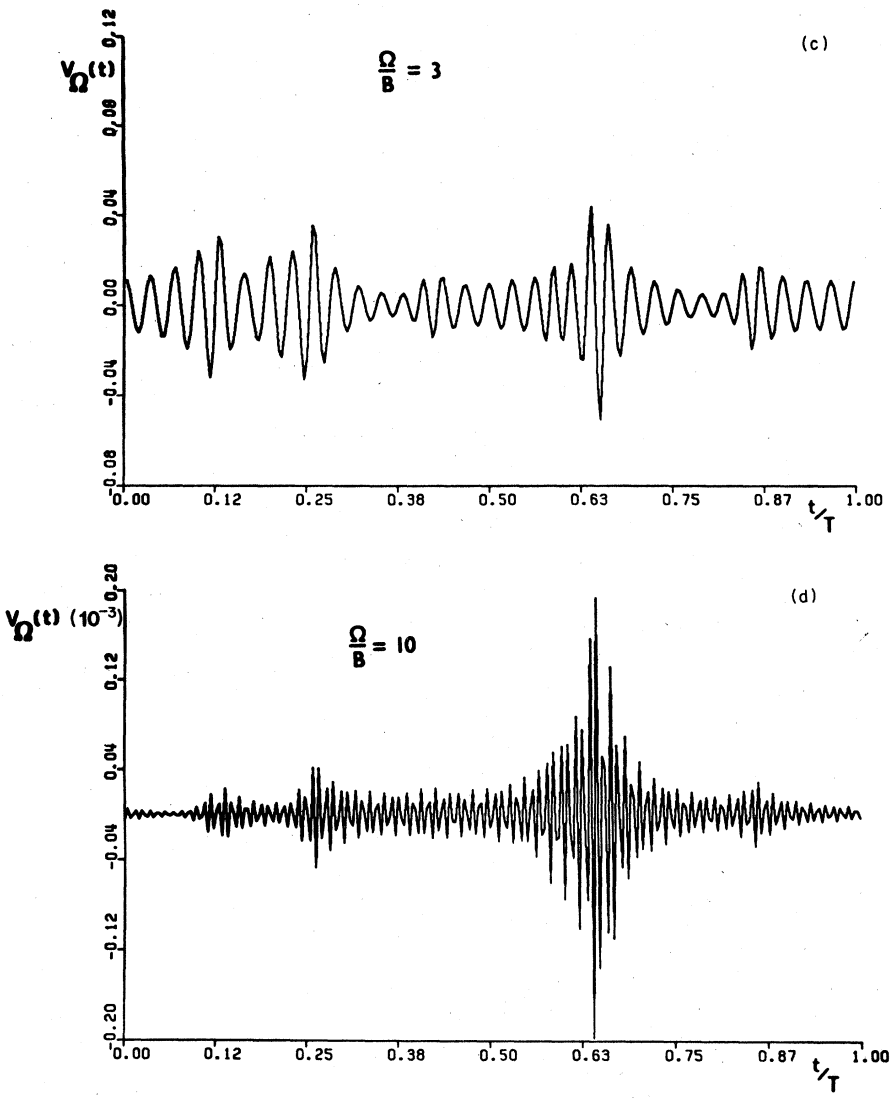

FIG. 4. *(Continued)*

The exponential factor $e^{\omega\tau}$ is bounded in ω (because the band is limited) and does not spoil the convergence of the Fourier integral for complex times. Equation (2.25) defines an entire random function, i.e., each realization is holomorphic for any complex z. It is also useful to think of $f(t+i\tau)$ as a complex-valued random function of two real variables t and τ, stationary in t. The correlation function is

$$\langle f(t+i\tau)f^*(t'+i\tau')\rangle = \int_{-B}^{+B} e^{-i\omega(t-t')}\, e^{+\omega(\tau+\tau')}\, \hat{\Phi}(\omega)\frac{d\omega}{2\pi}, \tag{2.26}$$

where $\hat{\Phi}$ is the spectrum of the force. In the Gaussian case, $f(z)$ is completely characterized by this correlation function; a limited band is not required to ensure convergence of the integral in (2.26); it suffices that $\hat{\Phi}(\omega)$ decrease faster than exponentially. If $\hat{\Phi}(\omega)$ decreases as $e^{-\alpha|\omega|}$ $(\alpha>0)$, the analytic continuation by the Fourier integral will give a random holomorphic function in the strip $|\mathrm{Im}(z)|<\alpha/2$. The case of non-band-limited forces will be briefly discussed in Sec. V B.

Analytic continuation of the solution of the NLL equation

The NLL equation is a nonlinear holomorphic ordinary differential equation (ODE), i.e., of the form $dv/dz = \mathcal{K}(z,v)$ where $\mathcal{K}$ is holomorphic in both z and v. It is actually an entire function of z, since the explicit z dependence is only through

the force, and an algebraic (cubic) function of v.

ODE's in the complex domain have been extensively studied during the late nineteenth and early twentieth centuries. An excellent review may be found in the recent book by Hille.[30] We have also found useful material in Davis's book.[31] What we need for the present investigation is fairly elementary and will now be briefly outlined.

Let us assume that the NLL equation has already been solved in the real-time domain (with suitable boundary conditions). Through successive differentiations we can determine all derivatives $v^{(n)}(t)$ of the velocity at any real t. By the Cauchy-Kowalewska theorem,[32] for times sufficiently close to t the solution can be represented by its Taylor series at t. The same series can be extended to complex times

$$v(z) = \sum_0^\infty \frac{1}{n!}\, v^{(n)}(t)(z-t)^n. \tag{2.27}$$

Convergence holds for $|z-t| < r(t)$, where $r(t)$, the radius of convergence, is the distance from t to the nearest singularity in the complex plane.[33]

By the Weierstrass analytic continuation method, the solution can then be continued to arbitrary nonsingular complex times.[34,35] The Weierstrass continuation requires that the Taylor coefficients be recalculated at successive points $z_1, z_2, \ldots$ such that $|z_{i+1} - z_i|$ is less than the distance from z_i to the nearest singularity. We also recall that analytic continuation from z_0 to z_F along two different paths produces the same result if either (i) the two paths can be continuously deformed into each other without crossing a singularity, or (ii) the solution is meromorphic, i.e., has only pole singularities. If, however, there are branch points (as is the case of the NLL equation), then different paths may lead to different results, corresponding to different sheets of the Riemann surface.[34] As a consequence of these multiple values the analytic continuation $v(t + i\tau)$ of a solution $v(t)$, periodic on the real axis, will not be periodic in t when $|\tau|$ exceeds the imaginary part of the singularity closest to the real axis (see Appendix B). The analytic continuation along a given path is easily implemented numerically using the Taylor expansion method described in Appendices A and B. Since only a finite number of derivatives are used (typically 10 to 100) it is a great advantage to be able to calculate the successive derivatives using the differential equation and not just the preceding Taylor series (equivalence of the two procedures follows from one of Painlevé's theroems[30]). The knowledge of high-order derivatives allows us to locate the nearest singularity very precisely by calculating ratios of successive derivatives without any need to integrate numerically very close to the singularity. Indeed, let $v(z)$ have a singularity at z_* with exponent ρ. Near z_* we have

$$v(z) = h_1(z) + (z - z_*)^\rho h_2(z), \tag{2.28}$$

where h_1 and h_2 are holomorphic in some neighborhood D of z_* and $h_2(z_*) \neq 0$. In the neighborhood of any $z_0 \in D$ (other than z_*) we have a Taylor series representation

$$v(z) = \sum_0^\infty A_p (z - z_0)^p. \tag{2.29}$$

It is then easily checked that for large p,

$$A_p / A_{p+1} = z_*[1 + (\rho + 1)/p + O(p^{-2})]. \tag{2.30}$$

Note that (2.30) is also valid for a logarithmic singularity (with $\rho = 0$). For examples of numerical implementation see Appendix B.

Nature of singularities

The singularities of an ODE are called "fixed" when their position is independent of initial conditions. Otherwise they are "movable." The solution of $dv(z)/dz = 1/z$ has a fixed logarithmic singularity at the origin. The solution of

$$\frac{dv}{dz} = -v^3; \quad v(z_0) = v_0, \tag{2.31}$$

which is

$$v(z) = \pm\,(2z + v_0^{-2})^{-1/2}, \tag{2.32}$$

has a movable branch point with exponent $-\frac{1}{2}$ at

$$z_* = -v_0^{-2}/2. \tag{2.33}$$

The position of movable singularities may be very hard to obtain when the ODE cannot be solved by quadrature (such as is the case for the NLL equation with arbitrary force). We can, however, very easily obtain the nature (for example the exponent) of the movable singularities, assuming they exist. Let us explain how this is done for the case of the NLL equation, written now in the complex domain

$$m\frac{dv(z)}{dz} = -\gamma v - v^3 + f(z). \tag{2.34}$$

With our assumptions $f(z)$ is an entire function. Hence, $f(z)$ and all its derivatives are bounded for any z. At a singular point z_* the velocity $v(z_*)$ or some derivative $dv^{(n)}(z_*)/dz^n$ must become infinite. Actually, $v(z_*)$ itself must be infinite; otherwise, by successive differentiation we see that all derivatives at z_* are finite. As z approaches z_* it is clear that the linear-γv term and the force

term in the NLL equation become "irrelevant." To leading order the NLL equation reduces to

$$m\frac{dv}{dz}\simeq -v^3;\quad v(z_*)=\infty. \tag{2.35}$$

Hence,

$$v(z)\simeq\left(\frac{2}{m}(z-z_*)\right)^{-1/2}. \tag{2.36}$$

We see that the movable singularities are branch points of exponent $-1/2$.

Position of singularities

The NLL equation has no fixed singularities at finite distance. The position of the movable branch points are, in principle, well determined by the boundary condition but are difficult to calculate analytically for arbitrary f. In Sec. II D we shall show that the probabilistic assumptions about f allow us to determine the "most relevant" singularities by a singular perturbation expansion. Here we limit ourselves to deterministic forces.

Let us assume that the force is periodic. In the spectral representation (2.3) we substitute a complex time $t+i\tau$ and assume that τ is very large positive. The Fourier sum is then dominated by the term with the largest frequency ω_M,

$$f(t+i\tau)\simeq\hat{f}_M e^{\omega_M\tau}e^{-i\omega_M t};\quad \tau\to\infty. \tag{2.37}$$

Using this in the NLL equation we find that $v(z)$ has an asymptotic expression with leading term $(\tau\to\infty)$

$$v(t+i\tau)\simeq\hat{f}_M^{1/3}e^{\omega_M\tau/3}e^{-i\omega_M t/3}. \tag{2.38}$$

Since the expression is nonsingular (except at infinity) it seems plausible that $v(z)$ has no singularities for sufficiently large τ.

When the coefficient m is small, information on the position of the singularities may be obtained by first considering the case $m=0$, where the NLL equation degenerates into an algebraic equation

$$0=-\gamma v-v^3+f(z). \tag{2.39}$$

For fixed z this cubic equation will generally have three distinct complex roots (only one real root for real t). At exceptional points where the equation has an n-fold multiple root ($n=2$ or 3), the solution has a branch point of exponent $1/n$. The double roots ($n=2$) are given by the discriminental equation

$$4\gamma^3+27f^2(z_*)=0, \tag{2.40}$$

or

$$f(z_*)=\pm i(4\gamma^3/27)^{1/2}. \tag{2.41}$$

We see that the branch points are determined by an equation which, for a given realization of the force, will generally be transcendental. Triple roots ($n=3$) are possible only if $\gamma=0$; they are then located at the zeros of f. If f is a typical realization of a zero-mean-value random function there will be such zeros on the real axis. For small m it appears that the NLL equation has singularities located close to those of the algebraic equation, although with a different exponent. For $\gamma=0$ this can be shown by a singular perturbation expansion closely related to what we shall present in Sec. II D; the displacement of the singularity is then proportional to $m^{3/5}$. For $\gamma>0$ the singular perturbation expansion has difficulties which we have not completely resolved. It seems likely that each singularity of the algebraic equation splits into a cloud of singularities of size $O(m^{2/3})$. This is stated tentatively and will not be used subsequently.

The easiest method to locate singularities is to integrate the NLL equation numerically with the Taylor expansion method of Appendix B and then to use high derivative ratios as explained above. This technique is applied to the case studied in the real domain at the end of Sec. II A. Figure 5(a) shows the position of the ten singularities in the upper half-plane closest to the real axis. For comparison, in Fig. 5(b), we show again a high-pass filtered velocity as a function of real time. It is seen that the high-frequency bursts are centered at the real part of the singularities closest to the real axis. Why this is so will be explained in Sec. II C.

C. Singularities and high-frequency behavior

We show in this section that the complex-time singularities of $v(z)$ determine the high-frequency behavior on the real axis. This is a classical result about Fourier transforms of analytic functions which is described in many textbooks. An elementary discussion with illuminating examples may be found in Ref. 36. Here is a brief outline of the ideas, mostly following Ref. 35. We assume that the function $v(t)$, which is real nonsingular for real t, has an analytic continuation $v(z)$ with singularities of exponent ρ at $z_j=t_j+i\tau_j$ and can be expressed in the neighborhood of z_j by

$$v(z)=(z-z_j)^\rho\sum_{p=0}^{\infty}a_{j,p}(z-z_j)^p+h, \tag{2.42}$$

where h denotes holomorphic terms. We also assume that $v(z)$ grows at most exponentially at infinity. Let us evaluate the Fourier transform

$$\hat{v}(\omega)=\int_{-\infty}^{+\infty}e^{i\omega t}v(t)\,dt, \tag{2.43}$$

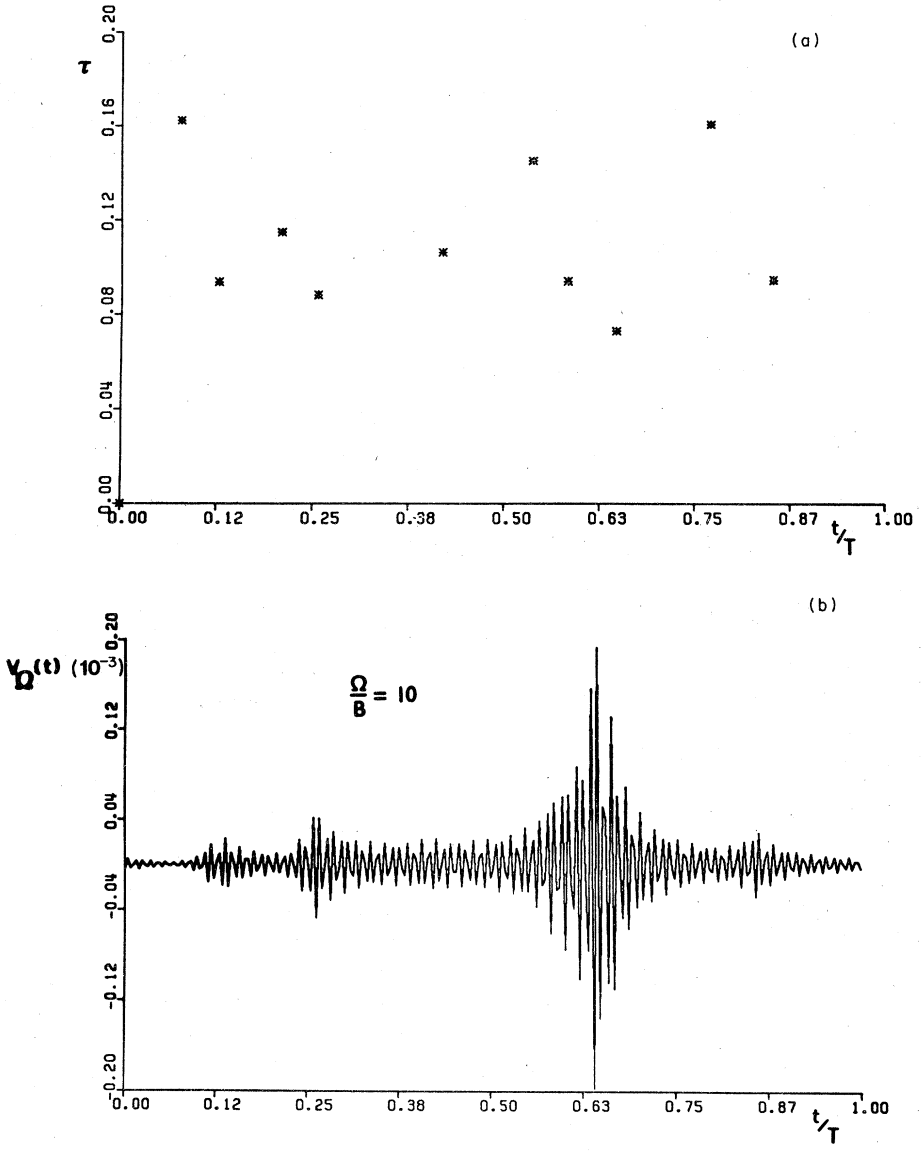

FIG. 5. Connection between bursts and complex-time singularities. (a) shows the position of the ten singularities in the upper half-plane closest to the real axis of the solution displayed in Fig. 4. (b) shows again the high-pass filtered velocity of Fig. 4(d). Note the correspondence between the position of the burst and the real part of the corresponding singularity. Note also that singularities which are closer to the real-time axis are associated with stronger bursts.

for $\omega \to +\infty$ (Hermitian symmetry gives then the $\omega \to -\infty$ values). We can shift the contour of integration away from the real axis so that it becomes the union of $\mathcal{C}_1$, $\mathcal{C}_2$, $\mathcal{C}_3, \ldots$ which wrap the singularities on the upper half-plane $\mathrm{Im}\, z > 0$ as shown in Fig. 6. The oscillatory exponentials in the Fourier integral are now converted into damped exponentials so that Laplace's method can be used for the asymptotic expansion. The final result is[35]

$$\hat{v}(\omega) \underset{\omega \to +\infty}{\simeq} -\frac{2\sin\pi\rho}{\omega^{\rho+1}} e^{-i\pi\rho/2} \sum_j^{\mathrm{up}} \epsilon_j e^{i\omega z_j} \sum_{p=0}^{\infty} a_{j,p}\, i^p \frac{\Gamma(\rho+p+1)}{\omega^p}, \tag{2.44}$$

where the summation over singularities is restricted to the upper half-plane. The ϵ_j's are determination factors. For the case of interest to us

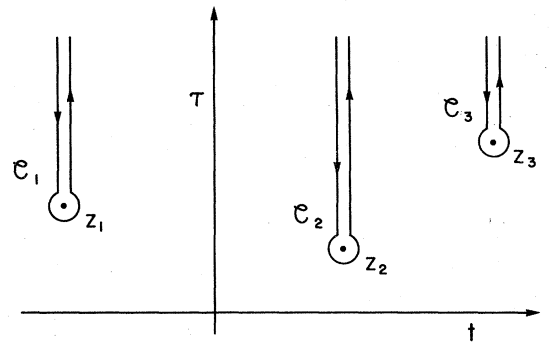

FIG. 6. Integration contour around singularities in the complex-time plane.

$$\rho=-\tfrac{1}{2},\quad \epsilon_j=\pm 1,\quad a_{j,0}=\left(\frac{m}{2}\right)^{1/2} \tag{2.45}$$

[cf. Eq. (2.36)]. Keeping only the leading term in the expansion, we obtain

$$\hat{v}(\omega)_{\omega\to+\infty}\simeq \sqrt{m/2}\ \Gamma(\tfrac{1}{2})e^{i\pi/4}\omega^{-1/2}\sum_j{}^{\rm up}\epsilon_j e^{i\omega z_j}. \tag{2.46}$$

We see that each singularity at z_j in the upper half-plane produces in the Fourier transform a complex exponential $e^{i\omega z_j}$ with a power-law prefactor $\omega^{-1/2}$. Notice that the exponential is controlled by the position of the singularity whereas the prefactor depends only on the exponent.

Intermittent bursts and singularities

From the asymptotic expansion (2.46) we can calculate the high-pass filtered velocity. Using (2.10) and (2.46) we obtain

$$v_\Omega(t)\underset{\Omega\to\infty}{\simeq} 2\,\mathrm{Re}\left(\int_\Omega^\infty e^{-i\omega t}\sqrt{m/2}\ \Gamma(\tfrac{1}{2})e^{i\pi/4}\omega^{-1/2}\sum_j{}^{\rm up}\epsilon_j e^{i\omega z_j}\frac{d\omega}{2\pi}\right)$$
$$\simeq \frac{\Gamma(\frac{1}{2})}{\pi}\left(\frac{m}{2}\right)^{1/2}\Omega^{-1/2}\sum_j{}^{\rm up}\epsilon_j e^{-\Omega\tau_j}\,\mathrm{Re}\left(\frac{\exp[-i\Omega(t-t_j)-i\pi/4]}{t-z_j}\right). \tag{2.47}$$

$v_\Omega(t)$ has an interesting structure. It is a linear superposition of bursts associated to individual singularities $z_j=t_j+i\tau_j$. Each burst is a modulated sine wave of frequency Ω. The modulation envelope is centered at the real part t_j of the singularity and decreases inversely proportional to the separation from center. There is an overall amplitude factor $\Omega^{-1/2}e^{-\Omega\tau_j}$ which favors the singularities close to the real axis. Two singularities at $z_1=t_1+i\tau_1$ and $z_2=t_2+i\tau_2$ ($\tau_2>\tau_1$) will produce well-separated bursts only if

$$|t_1-t_2|\gg\tau_2 e^{\Omega(\tau_2-\tau_1)}. \tag{2.48}$$

Otherwise, only the t_1-centered burst will be visible. We have thus understood the origin of the correspondence, observed in Figs. 5(a) and 5(b), between intermittent bursts and complex-time singularities located close to the real axis.

We are now in a position to give a qualitative picture of how unlimited intermittency arises in the present context. Let us first see what happens when we restrict our attention to a finite time interval. As we increase the filter frequency Ω, according to Eq. (2.48), the number of separated bursts will decrease until, eventually, a single burst remains, which corresponds to the singularity with smallest imaginary part τ. The center and amplitude of the corresponding burst will fluctuate randomly from realization to realization. The amplitude varies (roughly) like $e^{-\Omega\tau}$. For any continuous distribution of τ, this amplitude becomes increasingly intermittent as $\Omega\to\infty$. With an infinite time interval, which we can subdivide into nearly independent finite intervals, (we assume that the solution is mixing), the above result implies the following: as $\Omega\to\infty$ an ever smaller fraction of the intervals will remain "active." Note that our argument does not require that singularities come arbitrarily close to the real axis. Quantitative implementation of the above ideas is however greatly facilitated if this is the case, as is guaranteed by assumption (F5) on the statistics of the force. This will be discussed in Sec. II D.

D. The most relevant singularities

In order to apply the ideas of Sec. II C to the calculation of high-frequency statistical quantities we need to know the distribution of singularities. This distribution depends on the statistics of the force, the precise relationship being unknown.[37] However, for the high-frequency behavior, the only relevant singularities are those close to the real axis which, as we shall show in the section, can be obtained by a singular perturbation expansion. We begin with some heuristic considerations. We assume for simplicity that the parameters m and γ are $O(1)$. Typical singularities will then have imaginary parts also $O(1)$. For occasional (real) times there can nevertheless

be strong excursions in the force (if allowed by the statistics) which may allow singularities much closer to the real axis. When the force is large the NLL equation is satisfied, to leading order by a balance between the cubic term and the force term. We then obtain

$$v(t) \simeq f^{1/3}(t), \tag{2.49}$$

where $f^{1/3}(t)$ is understood to be the real cubic root with the same sign as $f(t)$. From (2.49) we can estimate $v(t)/\dot{v}(t)$ and thereby the distance to the nearest singularity

$$\frac{v(t)}{\dot{v}(t)} \simeq 3\frac{f(t)}{\dot{f}(t)}. \tag{2.50}$$

The smallest values will be achieved when simultaneously $f(t)$ is small and $\dot{f}(t)$ is large. [This is where we need assumption (F5) of Sec. II A.] Of course the argument is circular since we had to assume at the start that $f(t)$ is large. This is an indication that a singular perturbation calculation with inner and outer expansions is needed.

Let s_0 be a real time such that

$$f(s_0) = 0; \quad |\dot{f}(s_0)| = w \gg 1. \tag{2.51}$$

w^{-1} is going to serve as small expansion parameter. In the neighborhood of s_0 we can Taylor expand the force

$$f(t) = (t - s_0)\dot{f}_0 + \frac{(t - s_0)^2}{2!}\ddot{f}_0 + O(t - s_0)^3, \tag{2.52}$$

where

$$\dot{f}_0 = \dot{f}(s_0), \quad \ddot{f}_0 = \ddot{f}(s_0). \tag{2.53}$$

In the Gaussian case it is easy to show that $\ddot{f}_0$ conditioned upon (2.51) has mean zero and dispersion $O(1)$ and is therefore $O(1)$. In the general case it seems plausible that $\ddot{f}_0 = O(w)$ (at most) can be derived from the assumption of $O(1)$ bandwidth. Assuming this to be the case we now substitute the expansion (2.52) into the NLL equation

$$m\dot{v} = -\gamma v - v^3 + (t - s_0)\dot{f}_0 + O(w(t - s_0)^2). \tag{2.54}$$

This is the starting point for outer and inner expansions near s_0.

Outer expansion

Balancing the cubic term with the lowest-order term in the force we obtain

$$v_{\text{outer}} \simeq (\dot{f}_0)^{1/3}(t - s_0)^{1/3}. \tag{2.55}$$

Checking the other terms in (2.54) we find that (2.55) is the leading term in the region

$$m^{3/5}w^{-2/5} \ll |t - s_0| \ll 1. \tag{2.56}$$

Inner expansion

We rescale the variables as follows,

$$t - s_0 = m^{3/5}w^{-2/5}\xi, \tag{2.57}$$

$$v_{\text{inner}}(t) = m^{1/5}w^{1/5}x(\xi). \tag{2.58}$$

Substituting into (2.54) we obtain

$$\frac{dx}{d\xi} = -x^3 + \xi - \gamma(mw)^{-2/5}x + O(m^{3/5}w^{-2/5}\xi^2). \tag{2.59}$$

The inner equation (all terms with negative power of w dropped) is

$$\frac{dx}{d\xi} = -x^3 + \xi. \tag{2.60}$$

Matching of the inner and outer expansions gives us the boundary conditions at large ξ

$$x(\xi) \simeq \xi^{1/3}, \quad \text{for } \xi \to \pm\infty. \tag{2.61}$$

In Appendix C we show that Eq. (2.60) with the boundary condition (2.61) has a unique real solution which is analytic on the real axis and exhibits singularities with exponent $-\frac{1}{2}$ in the complex domain. The ones closest to the real axis are located at

$$\zeta_* = \xi_* + i\eta_* \simeq 1.707\,907 + i\ 0.778\,600 \tag{2.62}$$

and at the complex conjugate location. In addition, we have found another pair of singularities at $\zeta_{**} \simeq 2.198\,79 \pm i\ 1.869\,63$ which, owing to their 2.4 times bigger imaginary part, do not contribute to the leading order of the high-frequency asymptotic expansion. In the original variables the position of the dominant singularity in the upper half-plane is given to leading order in w^{-1} by

$$z_* \simeq s_0 + m^{3/5}w^{-2/5}\zeta_*, \quad w = |\dot{f}_0|. \tag{2.63}$$

For large $|\dot{f}_0|$ this singularity is, as announced, close to the real axis.

Note that in the above derivation we have not made use of the boundary or initial conditions of the original NLL equation. Since we are calculating the position of a movable singularity, there must be some dependence on initial or boundary conditions. However, it may be shown that this dependence is through exponentially small terms in w which would not even affect higher orders in the expansion (2.63). Thus we see that a movable singularity has become asymptotically fixed.

Our analysis can be extended to the case of small m and γ which will be needed in Sec. II F. The singularities are then located in the neighborhood of all the zeros of $f(t)$ and not just those with large derivative.

(i) If $\gamma^{5/2} \ll m \ll 1$, all the preceding singular perturbation analysis remains valid. However, we can now use m as expansion parameter so

that the condition $w \gg 1$ is not needed.

(ii) If $m \ll \gamma^{5/2} \ll 1$, we see from (2.59) that the damping term is strongly relevant for $w = O(1)$. We expect (but have not proved rigorously) that the singularities of the NLL equation are close to those of the algebraic equation ($m = 0$). The latter are obtained from the discriminental equation (2.40) by expanding near the zeros of f, yielding to leading order in γ,

$$z_* = s_0 + i|\dot{f}_0|^{-1}\gamma^{3/2}(\tfrac{4}{27})^{1/2}. \tag{2.64}$$

E. The spectrum and the flatness

In this section we calculate the high-frequency behavior of the spectrum and the flatness. We assume throughout that m and γ are $O(1)$. The case of small m and γ will be examined in Sec. II F.

In each realization the high-frequency Fourier components are given in terms of the singularities by (2.46) and the singularities are given by (2.63). Before presenting a detailed calculation let us sketch the main steps in a heuristic way. For this we restrict ourselves to the Gaussian case and ignore algebraic prefactors and inessential numerical constants. The singularities located near the zeros of $f(t)$ have imaginary parts $\sim w^{-2/5}$, where w is the absolute value of the derivative of f. Each singularity produces an exponential damping of the form $\exp(-\omega w^{-2/5})$. The spectrum is therefore an average of $\exp(-2\omega w^{-2/5})$ weighted with a Gaussian distribution for w. Thus the spectrum behaves like $\exp(-c\omega^{5/6})$ at large ω's. Similarly, the fourth-order moment $\langle v_\Omega^4 \rangle$, involving an average of $\exp(-4\Omega w^{-2/5})$ behaves like $\exp[-c(2\Omega)^{5/6}]$. Hence, for the flatness we have $F(\Omega) \sim \exp[c(2-2^{5/6})\Omega^{5/6}]$; this implies unlimited intermittency. Let us now turn to the actual calculation.

The spectrum

The velocity spectrum $E(\omega)$ is defined in terms of the Fourier transform of the velocity by

$$\langle \hat{v}(\omega)\hat{v}(\omega') \rangle = 2\pi\delta(\omega+\omega')E(\omega). \tag{2.65}$$

It is easily shown that

$$E(\omega) = \lim_{L\to\infty} \frac{1}{L} \langle \hat{v}_L(\omega)\hat{v}_L(-\omega) \rangle, \tag{2.66}$$

where $\hat{v}_L(\omega)$ is the Fourier transform of the restriction of $v(t)$ to the interval $[0, L[$. From (2.46) we know that for $\omega \to +\infty$,

$$\hat{v}_L(\omega) \simeq (m/2)^{1/2}\Gamma(1/2)\, e^{i\pi/4}\omega^{-1/2}\sum_j^{\text{up}}{}_L\, \epsilon_j e^{i\omega z_j}, \tag{2.67}$$

where the summation is over all singularities in the upper half-plane with real part between 0 and L. The location of the singularities are given by (2.63).

$$z_j \simeq s_j + m^{3/5} w_j^{-2/5}(\xi_* + i\eta_*), \tag{2.68}$$

where the s_j's are the real zeros of $f(t)$ and $w_j = |\dot{f}(s_j)|$. Substitution of (2.67) into (2.66) produces a double summation, say over indices j and l. In this summation the terms with $j \neq l$ do not contribute to the leading order of the average (for $\omega \to \infty$) essentially because of additional phase mixing from averaging over $e^{i\omega(s_j - s_l)}$. This is best checked after the $j = l$ contributions have been evaluated. In the latter the phase factors drop out and we are left with

$$E(\omega) \simeq \lim_{L\to\infty} \frac{1}{L}\frac{m}{2}\Gamma^2(\tfrac{1}{2})\omega^{-1}\left\langle \sum_j^{\text{up}}{}_L \exp(-2\omega m^{3/5} w_j^{-2/5}\eta_*) \right\rangle. \tag{2.69}$$

The summation over the zeros of $f(t)$ can be transformed into an integral using the identity

$$\delta(f(t))|\dot{f}(t)| = \sum_j \delta(t - s_j). \tag{2.70}$$

The average is then expressed in terms of the joint probability density of f and $\dot{f}$. The latter is expressible in terms of $p(0)$, the probability density of $f = 0$, and $Q(w)$, the conditional probability density of the absolute values of $\dot{f}$ when $f = 0$. In the Gaussian case

$$Q(w) = 2(2\pi)^{-1/2} e^{-w^2/2}. \tag{2.71}$$

To investigate also non-Gaussian cases without aiming for total generality (we wish to be able to perform the asymptotic expansion of the spectrum as explicitly as possible) we allow the following one-parameter form for $Q(w)$,

$$Q(w) = C_\alpha \exp(-w^{2\alpha}/2), \quad \alpha > 0. \tag{2.72}$$

We then obtain

$$E(\omega) \simeq \frac{m}{2}\Gamma^2(\tfrac{1}{2})p(0)C_\alpha\omega^{-1} \times \int_0^\infty dw\, w \exp\left(-\frac{w^{2\alpha}}{2} - 2\omega m^{3/5} w^{-2/5}\eta_*\right). \tag{2.73}$$

For large ω the integral is evaluated by Laplace's method. The final result is ($\omega \to +\infty$)

$$E(\omega) \simeq A_\alpha m^{(7\alpha+8)/(10\alpha+2)}\omega^{(8-15\alpha)/(10\alpha+2)} \times \exp[-B_\alpha(\omega m^{3/5})^{5\alpha/(5\alpha+1)}], \tag{2.74}$$

where

$$A_\alpha = \frac{\sqrt{2\pi}}{4}\Gamma^2(\tfrac{1}{2})p(0)C_\alpha\left(\frac{\alpha(5\alpha+1)}{10}\right)^{-1/2} \times\left(\frac{4\eta_*}{5\alpha}\right)^{(10-5\alpha)/(10\alpha+2)}, \quad (2.75)$$

$$B_\alpha = \frac{5\alpha+1}{2}\left(\frac{4\eta_*}{5\alpha}\right)^{5\alpha/(5\alpha+1)}. \quad (2.76)$$

The Gaussian case ($\alpha = 1$) is

$$E(\omega) \simeq A_1 m^{5/4}\omega^{-7/12}\exp[-B_1(\omega m^{3/5})^{5/6}], \quad (2.77)$$

$$A_1 = \frac{1}{2\sqrt{2\pi}}\Gamma^2(\tfrac{1}{2})(\tfrac{5}{3})^{1/2}\left(\frac{4\eta_*}{5}\right)^{5/6}, \quad (2.78)$$

$$B_1 = 3\left(\frac{4\eta_*}{5}\right)^{5/6}. \quad (2.79)$$

Let us now comment on the results. Although each individual singularity produces an ordinary exponential damping, the averaging will give a somewhat slower than exponential damping because in the statistical ensemble the singularities with very small imaginary part produce very slow damping. The power-law prefactors of the exponential ($\omega^{-7/12}$ in the Gaussian case) are due to the combined effects of the $\omega^{-1/2}$ prefactors of individual singularities (a signature of the nature of the singularity) and of the distribution of singularities.

We particularly emphasize the *absence of universality* of the spectrum with respect to changes in the statistics of the force (materialized by changing α). Such changes cannot be absorbed in scaling factors since they actually modify the exponents both of the arguments of the exponentials and of the prefactors. Further comments on this are postponed to Sec. V A.

The flatness

We wish to calculate, for filter frequencies $\Omega \to \infty$,

$$F(\Omega) = \langle v_\Omega^4\rangle / \langle v_\Omega^2\rangle^2. \quad (2.80)$$

The denominator is expressible in terms of the spectrum

$$\langle v_\Omega^2\rangle = \int_{|\omega|\geq\Omega} E(\omega)\, d\omega/(2\pi). \quad (2.81)$$

The numerator is expressible as

$$\langle v_\Omega^4\rangle = \lim_{L\to\infty}\frac{1}{L}\iiiint_{|\omega_{1,2,3,4}|\geq\Omega}\langle\hat{v}_L(\omega_1)\hat{v}_L(\omega_2)\hat{v}_L(\omega_3)\hat{v}_L(\omega_4)\rangle\,\frac{d\omega_1}{2\pi}\frac{d\omega_2}{2\pi}\frac{d\omega_3}{2\pi}\frac{d\omega_4}{2\pi}, \quad (2.82)$$

where $\omega_4 = -\omega_1-\omega_2-\omega_3$. There are a number of possibilities which fall into two groups (I) $\omega_1,\omega_2 \geq \Omega$, $\omega_3,\omega_4 \leq -\Omega$ plus permutations (II) $\omega_1,\omega_2,\omega_3 \geq \Omega$, $\omega_4 \leq -3\Omega$ plus permutations. The second group does not contribute to the leading order of $\langle v_\Omega^4\rangle$. The evaluation of $F(\Omega)$ proceeds along exactly the same lines as for the spectrum. Again the leading order comes from taking the same singularity several times (four times now). The final result is ($\Omega \to \infty$)

$$F(\Omega) \simeq \mathfrak{A}_\alpha m^{-3(\alpha+2)/(10\alpha+2)}\Omega^{(5\alpha-8)/(10\alpha+2)} \times\exp[\mathfrak{B}_\alpha(\Omega m^{3/5})^{5\alpha/(5\alpha+1)}], \quad (2.83)$$

where $\mathfrak{A}_\alpha$ is a positive pure numerical constant which we do not need and

$$\mathfrak{B}_\alpha = \frac{5\alpha+1}{2}\left(\frac{4\eta_*}{5\alpha}\right)^{5\alpha/(5\alpha+1)}(2-2^{5\alpha/(5\alpha+1)}) > 0. \quad (2.84)$$

The Gaussian case is

$$F(\Omega) \simeq \mathfrak{A}_1 m^{-3/4}\Omega^{-1/4}\exp[\mathfrak{B}_1(\Omega m^{3/5})^{5/6}] \quad (2.85)$$

$$\mathfrak{B}_1 = 3\left(\frac{4\eta_*}{5}\right)^{5/6}(2-2^{5/6}). \quad (2.86)$$

Clearly, the flatness grows without bound as $\Omega \to \infty$. We have thus demonstrated unlimited intermittency without assuming a large Reynolds number [m and γ and the force are $O(1)$]. Kraichnan's conjectures[14] are thereby confirmed for the NLL model. Notice that the flatness displays the same kind of nonuniversality as the spectrum.

F. The high-Reynolds number limit

So far we assumed that m and γ were $O(1)$ and had only the frequency as expansion parameter. The case of very large m and/or γ (very small Reynolds numbers) is not of central importance in this paper. Qualitatively the situation is as follows. Owing to the strong damping, typical singularities occur very far from the real axis; occurences very close to the real axis have extremely small probabilities; as a consequence, the high-frequency intermittent regime described by Eqs. (2.74) and (2.83) is still present but rejected to extremely high frequencies.

We now discuss in more detail the case when both m and γ are small. The nonlinearity is then strong on the real axis, a situation analogous to the high-Reynolds number case for the Navier-Stokes equation. We shall show that the NLL model has then a universal inertial range with power-law behavior of both spectrum and flatness. As in Sec. II E, we begin with a heuristic approach.

With $m=\gamma=0$, the NLL equation becomes

$$-v^3(t)+f(t)=0. \tag{2.87}$$

The solution $v(t)=f^{1/3}(t)$ has high-frequency components even when $f(t)$ does not. Indeed, near a zero of the force, the velocity has an inflection point with vertical tangent (like $t^{1/3}$). This real-time singularity produces an $\omega^{-4/3}$ term in the Fourier transform. Hence $|\hat{v}(\omega)|^2$ and its average are expected to have an $\omega^{-8/3}$ dependence at high ω. The $f^{1/3}(t)$ solution is intermittent in the most immediate sense: all the high-frequency content comes from isolated points, the zeros of the force. To estimate the flatness we can identify $F^{-1}(\Omega)$ with the fraction of "active" time when the velocity is observed with temporal resolution Ω^{-1}. The time interval between successive zeros being $O(1)$ we find $F(\Omega)\sim\Omega$.

A more systematic derivation of the above results is now outlined, still assuming $m=\gamma=0$. Calculating the Fourier transform of an individual real-time singularity

$$v(t)\simeq(\dot{f}_0)^{1/3}(t-s_0)^{1/3}, \tag{2.88}$$

we obtain for $\omega\to\infty$,

$$\hat{v}(\omega)\simeq i\Lambda(\dot{f}_0)^{1/3}e^{i\omega s_0}\omega^{-4/3}, \tag{2.89}$$

$$\Lambda=\tfrac{4}{9}\int_0^\infty dx\,x^{-5/3}\sin x.$$

Summing over all singularities in the interval $[0,L[$ and using the same notation and mostly the same arguments as in Sec. II E, we find

$$E(\omega)\simeq\Lambda^2|\omega|^{-8/3}\lim_{L\to\infty}\frac{1}{L}\int_0^L\langle\dot{f}^{2/3}(t)\delta(f(t))|\dot{f}(t)|\rangle dt$$

$$\simeq\Lambda^2 p(0)\int_0^\infty dw\,w^{5/3}Q(w)|\omega|^{-8/3}. \tag{2.90}$$

This power-law spectrum is universal because the statistics of the force enters only through the numerical prefactor. The calculation of the flatness proceeds exactly along the same lines and gives us the expected power law for $\Omega\to\infty$,

$$F(\Omega)\sim\Omega. \tag{2.91}$$

The flatness result is even more universal than the spectrum: If the cubic term in the NLL equation is changed to v^5, the spectrum changes to $|\omega|^{-12/5}$ but the flatness is unchanged.

We turn now to the case of small but nonzero m and/or γ. The presence of either the time derivative or the damping pushes the real-time singularities into the complex domain while changing their exponents from $\frac{1}{3}$ to $\frac{1}{2}$ or $-\frac{1}{2}$. The discussion at the end of Sec. II D shows that two cases must be distinguished.

(i) If $\gamma\ll m^{2/5}\ll 1$, the presence of the damping is irrelevant at high frequencies. The singularities have exponents $\rho=-\frac{1}{2}$ and are located $O(m^{3/5})$ from the real axis and are therefore felt at frequencies greater or equal to the "dissipation frequency"

$$\omega_D\sim m^{-3/5}. \tag{2.92}$$

Above ω_D we can use the asymptotic expansions [(2.74) and (2.83)] for the spectrum and the flatness. A useful check on the calculation is that these results and those of the $m=\gamma=0$ case are found to match at $\omega\sim\omega_D$.

(ii) If $m^{2/5}\ll\gamma\ll 1$, the square root singularities of the $m=0$ equation, which are located $O(\gamma^{3/2})$ from the real axis will be strongly felt in the "intermediate dissipation range"

$$\omega_D'\sim\gamma^{-3/2}\ll|\omega|\ll\omega_D. \tag{2.93}$$

In this range we cannot use the results of Sec. II E. Redoing the calculation with a different type of singularity, we find that the spectrum behaves like $\exp(-C_1\gamma|\omega|^{2/3})$ and the flatness like $\exp(C_2\gamma\Omega^{2/3})$. C_1 and C_2 are positive numerical constants; we have ignored power-law prefactors.

To summarize, the inertial-range expressions (2.90) and (2.91) are valid for

$$1\ll|\omega|\ll\inf(\omega_D,\omega_D'). \tag{2.94}$$

"Inertial" is the proper name for such a range since the dynamics are controlled solely by the nonlinear term. Indeed, the force is limited to $O(1)$ frequencies and the dissipative terms ($-\gamma v$ and $m\dot{v}$) are negligible.

Finally, the existence of the inertial range is checked numerically by a Monte Carlo simulation. We take $m=0.003\,74$, $\gamma=0.001$, a Gaussian periodic force with seven modes and flat spectrum. Averaging is done over 20 realizations (see Ap-

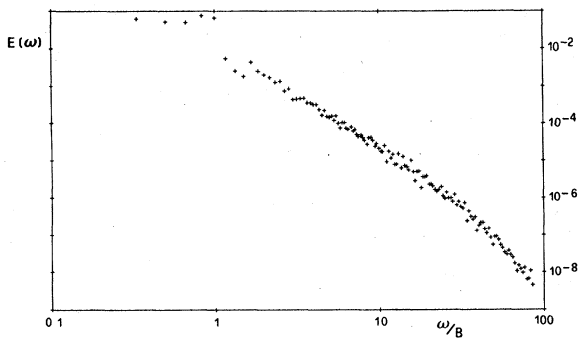

FIG. 7. "High-Reynolds number" spectrum. The log-log plot shows the results of numerical solution of the NLL with $\gamma=10^{-3}$ and $m=0.003\,74$ and a Gaussian force with seven modes. Notice the distinct $\omega^{-8/3}$ range.

pendix A). The resulting spectrum, shown in Fig. 7 has a distinct $\omega^{-8/3}$ range.

G. Comparison with closure

In the context of turbulence "closure" means generally any heuristic procedure whereby a finite system of equations is obtained for suitably chosen mean quantities. Reviews of closure procedures for homogeneous turbulence may be found in Refs. 38–41. Closures of the so-called Markovian kind deal only with single time quantities and are not adequate for our purposes. A potentially more interesting class of closures are those based on field-theoretic renormalized perturbation expansions.[42] For Gaussian random forces such closures may be viewed as partial resummations of graphs contributing to the n-point cumulants and response functions. Perturbation terms of arbitrary high orders are included making nontrivial high-frequency behavior possible. In this section we discuss the case of the direct interaction approximation (DIA), the simplest self-consistent field theoretic procedure.[24]

The NLL equation in integral form with initial conditions at $-\infty$ reads

$$v(t)=\int_{-\infty}^{t}\exp[-\gamma(t-t')/m]\,[f(t')-v^3(t')]\,dt'/m. \tag{2.95}$$

We rewrite this in graphical form as

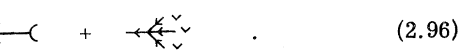

(2.96)

The unperturbed response function $\exp[-\gamma(t-t')/m]$ is represented by ⟵ ; ⟵○ stands for f/m and  is the cubic vertex. The DIA makes use of the response function

$$G(t,t')=\frac{1}{m}\,\langle\delta v(t)/\delta f(t')\rangle=$$ 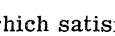 , (2.97)

which satisfies the causality condition

$$G(t,t')=0,\quad \text{for } t<t', \tag{2.98}$$

and of the correlation function

$$U(t,t')=\langle v(t)v(t')\rangle=$$ 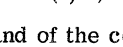 . (2.99)

Stationarity allows us to write these as functions of $t-t'$ only, denoted $G(t-t')$ and $U(t-t')$. The DIA equations are obtained by writing the Dyson equation for the self-energy and then replacing the four-point vertex function by the bare vertex. In graphical form they read

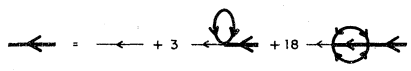

(2.100)

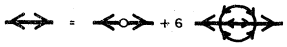

(2.100′)

where —○— stands for the correlation of $f(t)/m$. The DIA equation may also be obtained as the $N\to\infty$ limit of the random coupling model[43,44]

$$m\dot v_\alpha=-\gamma v_\alpha-\frac{1}{N}\sum_\beta v_\beta v_\beta v_\alpha-\frac{1}{N}\sum_{\beta,\gamma,\delta}\Phi_{\alpha\beta\gamma\delta}v_\beta v_\gamma v_\delta+f_\alpha(t)\,. \tag{2.101}$$

The $\Phi_{\alpha\beta\gamma\delta}$'s $(\alpha,\beta,\gamma,\delta=1,\ldots,N)$ are a set of zero mean-value and unit-variance Gaussian random variables completely symmetric in $\alpha,\beta,\gamma,\delta$ but otherwise independent. The f_α's are N independent versions of the force. As long as (2.100) and (2.101) have a unique solution the model ensures the realizability of the DIA equation, i.e., the positivity of the energy spectrum.

In explicit notation the DIA equations read

$$\frac{dG(t)}{dt}+\frac{\gamma+3U(0)}{m}G(t)=\frac{18}{m^2}\int_0^t G(t-t')U^2(t-t')G(t')dt',\quad \text{for } t\geq 0;\quad G(0)=1 \tag{2.102}$$

$$U(t)=\frac{1}{m^2}\int_0^\infty dt_2\int_0^\infty dt_1 G(t_2)G(t_1)[\Phi(t-t_2+t_1)+6U^3(t-t_2+t_1)]\,. \tag{2.102′}$$

The best way to study the high-frequency behavior of the spectrum is to apply to the DIA equations the same analytic function techniques as to the "primitive" NLL model. There is a major simplification that comes from using closure (any closure): Once the nature and positions of the complex-time singularities are obtained, the high-frequency behavior follows without further averaging. For example, if we know that the singularity of $U(t+i\tau)$ in the upper half-plane, closest to the real axis is at z_* with exponent ρ, then for $\omega\to+\infty$ the spectrum is

$$E(\omega)\sim\omega^{-\rho-1}\exp(i\omega z_*)\,. \tag{2.103}$$

The positivity constraint implies that the singularity must be on the imaginary-time axis.

There are also new difficulties associated with the complex time DIA. First, the response function, which satisfies the causality condition (2.98), is not analytic on the real-time axis and cannot be continued to complex times. Equivalently, it can be checked that its Fourier transform behaves algebraically, not exponentially, at high frequencies. Note, however, that it suffices to continue

the correlation function to complex times. This is done via Eq. (2.102′) which we have written in such a way that t can become complex while the arguments of the response functions stay real. Second, there is a problem of nonuniqueness. As discussed by Kraichnan in a somewhat similar context,[45] the DIA when applied to the NLL model does not really distinguish between a $-v^3$ and a $+v^3$ cubic term. There is a distinction stemming from the $3U(0)G(t)/m$ term but this can be absorbed in a renormalization of the damping γ. With $+v^3$ there is a possibility of self-excited solutions with zero force. These spurious solutions are also present when the force is "small" or, equivalently, when the force is $O(1)$ but γ is large (very low Reynolds numbers).[46]

The nature of the singularities of the DIA equations can be obtained by making an Ansatz $U(z) \sim (z - z_*)^\rho$ and then looking for the most divergent terms in (2.102′). As usual, the force $\Phi(z)$, which is an entire function, does not contribute. The U^3 term integrated over two time arguments gives $(z - z_*)^{3\rho+2}$. For this to balance the U term in the lhs we must have $\rho = -1$, i.e., a leading-order pole. This implies, provided there are no real-time singularities, that the spectrum will be a pure exponential for large ω,

$$E(\omega) \sim e^{-\tau_* |\omega|} . \tag{2.104}$$

At low Reynolds numbers, by perturbation calculation around the linear solution, one can construct a solution of the DIA equation which is analytic in a finite strip around the real axis. It seems plausible that this solution will have complex-time singularities. Thus, for high ω the spectrum will be exponential and universal with respect to the force. In contrast, for the exact NLL model, we know that there is no finite analyticity strip because singularities can come arbitrarily close to the real axis: also, the exact spectrum decreases as the exponential of minus some nonuniversal power of the frequency, depending on the force [Eq. (2.74)]. DIA and exact solution are thus always inconsistent at sufficiently high frequencies.[47] Going to higher orders of renormalized perturbation is unlikely to cure the discrepancy because this will just replace the deterministic DIA equations by a larger but finite set of deterministic equations which will presumably also have an analyticity strip around the real axis.

We finally come to the question of closure and intermittency. This requires the knowledge of four-point functions to evaluate the flatness. With no vertex corrections the fourth-order cumulant is given by the following graph

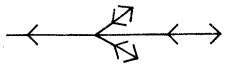

which involves one response and three correlation functions. A simple calculation using (2.104) shows that, for $\Omega \to \infty$, this cumulant has a negligible contribution to the flatness, which therefore reduces to its Gaussian value $F = 3$, implying no intermittency. A very similar calculation was done recently for the Navier-Stokes equation by Kuzmin.[48] Starting from the DIA solution he calculated the contribution to the flatness of the analog of the above graph as well as of higher-order ones; he concluded that intermittency disappears at high wave numbers. Clearly this is not so for the exact dynamics (at least for the NLL model). It can, however, not be ruled out that unlimited intermittency is obtained if one uses, instead of the DIA, a field theoretic approximation which self-consistently calculates moments up to fourth order, such as the vertex renormalized equations.[42]

III. INTERMITTENCY AND INTRINSIC STOCHASTICITY: THE LORENZ MODEL

Randomlike behavior in a nonlinear dynamical system can arise in at least two ways: The system can be driven by a prescribed random force such as is the case for the NLL model and thereby achieve extrinsic stochasticity. There are also systems governed by purely deterministic equations which display intrinsic stochasticity. Such behavior was demonstrated convincingly for the first time by Lorenz.[25] The Lorenz model is a system of ordinary differential equations

$$\begin{aligned} \dot{X} &= -\sigma X + \sigma Y , \\ \dot{Y} &= -XZ + rX - Y , \\ \dot{Z} &= XY - bz . \end{aligned} \tag{3.1}$$

For example, for $\sigma = 10$, $b = \frac{8}{3}$, and $r = 28$, as $t \to \infty$ the point $X(t), Y(t), Z(t)$ is attracted to a set with a Cantor-type structure, which presumably is a "strange attractor."[49] Randomness in real turbulent flows may, according to the cases, be achieved by extrinsic or intrinsic mechanisms or a mixture.[50] It has been pointed out by Ruelle[51] that random forces are not a prerequisite in modeling the chaotic aspect of turbulence. Furthermore, we have seen that random forces, even when restricted to low frequencies, will affect the high-frequency behavior, leading to nonuniversality in the dissipation range (but not in the inertial range).

It is now natural to ask if intrinsically stochastic systems such as the Lorenz model display high-

frequency intermittency. To avoid possible confusions we note that a different kind of low-frequency intermittency may be present in dynamical systems undergoing a bifurcation from nonstochastic to stochastic behavior.[52-54] According to Ref. 52, the short turbulent bursts sometimes observed just above the threshold reflect the fact that the subcritical state is still weakly attracting. Similar intermittency may be observed in systems undergoing transition from a stochastic state to a stochastic state with more degrees of freedom excited, e.g., the appearance of a magnetic field in a turbulent conducting fluid.[55] Although such turbulent bursts are conspicuous without high-pass filtering, associated phenomena have been observed involving complex-time singularities.[56]

The solutions of the Lorenz equations can be analytically continued to complex times by the method described in Sec. II B. An important difference with the NLL model is that the solution of Eqs. (3.1) is analytic in a finite strip around the real axis $0 \leq |\mathrm{Im}t| \leq \tau_{\mathrm{anal}}$. Indeed, it was shown by Lorenz,[25] using a simple energy estimate, that the attractor, whatever its precise nature, is bounded (in the real domain). This implies a (uniform in time) lower bound for the radius of convergence of the Taylor series at any real time. The nature of the (possible) singularities can be found by first eliminating the Y and Z variables, then substituting a constant times $(t-t_*)^p$ for the X variable and balancing the most singular terms. This gives, to leading order, pole singularities

$$X(t) \simeq \pm 2i(t-t_*)^{-1},$$
$$Y(t) \simeq \mp \frac{2i}{\sigma}(t-t_*)^{-2}, \tag{3.2}$$
$$Z(t) \simeq -\frac{2}{\sigma}(t-t_*)^{-2}.$$

However, the solutions are meromorphic only for exceptional values of the parameters.[57] In general, higher-order terms contain logarithmic corrections; natural boundaries can also not be ruled out.[56]

To check the existence of singularities we integrate the Lorenz equations in the stochastic regime ($\sigma = 10, b = 8/3, r = 28$), using the complex-time Taylor expansion method described in Appendix B. For the real initial conditions $X(0) = -5$, $Y(0) = -4, Z(0) = 25$, Table I gives the singularities with positive imaginary part less than 0.24 in the time interval $[0,10]$. We checked that the complex-time behavior is consistent with Eqs. (3.2). The positions of the singularities are very sensitive to initial conditions and, presumably, as random as the attractor itself. It would be of interest to determine the distribution $N(\tau)d\tau$ of

TABLE I. Complex-time singularities of the Lorenz Model.

Ret	Imt
0.409	0.231
1.066	0.222
1.734	0.213
2.419	0.202
3.136	0.188
3.940	0.168
4.685	0.177
5.628	0.153
6.956	0.204
7.664	0.191
8.438	0.174
9.246	0.167
9.979	0.181

singularities, i.e., the mean number of singularities per unit real time with positive imaginary part between τ and $\tau + d\tau$. From the existence of a finite analyticity strip we infer that the support of $N(\tau)$ has a positive lower bound $\tau_{\mathrm{min}} \geq \tau_{\mathrm{anal}}$. Numerical determination of $N(\tau)$ by simulation appears feasible. However, it would be very difficult to obtain the behavior in the immediate neighborhood or τ_{min}. In the absence of any genuine theory of the Lorenz attractor we do not see presently how to obtain $N(\tau)$ by analytic methods. However, there are results which do not require the precise knowledge of $N(\tau)$. First, for high ω we expect that the spectrum of any component of the solution behaves exponentially with possibly slower prefactors. This follows from the existence of a lower bound for the imaginary parts of singularities. Second, using the argument given at the end of Sec. IIC, we expect that, unless τ can take its lower bound value τ_{min} with a finite probability (a very unlikely situation), then the high-pass filtered solution will display unlimited intermittency.

The Lorenz model, contrary to the NLL model does not seem to have an interesting high-Reynolds number limit. Indeed, when the nonlinearity (measured by the Rayleigh number r) becomes too large, the solution has a limit cycle and thus loses stochasticity.[58] To achieve a modeling of true turbulence more realistic with respect to both intrinsic stochasticity and small-scale behavior, it would be of interest to find a dynamical system with a parameter r such that, for $r \to \infty$, intrinsic stochasticity remains while some singularities migrate to the real-time axis.

IV. SPATIAL INTERMITTENCY IN BURGERS'S MODEL

In this section we study the nonlinear partial differential equation

$$\frac{\partial v(t,x)}{\partial t}+\frac{1}{2}\frac{\partial}{\partial x}v^2=\nu\frac{\partial^2 v}{\partial x^2},\quad v(0,x)=v_0(x), \tag{4.1}$$

introduced by Burgers.[26] Owing to obvious stability properties Burgers's model, like the NLL model, displays no intrinsic stochasticity. Random behavior can be achieved either via random driving or via random initial conditions. We shall concentrate on the latter and assume that $v_0(x)$ satisfies the same conditions (F1)–(F4) in x space as the random force of the NLL model (condition (F5) is not required). Without external driving the solutions of Burgers's equation are decaying to the $v\equiv 0$ steady-state solution. We can, however, investigate, at a fixed time, the small-scale spatial behavior which is governed by singularities at complex space locations.

The analytic structure of individual solutions of Burgers's equation is well understood. This follows from the explicit representation obtained by Hopf and Cole.[59]

$$v(t,x)=-2\nu\frac{\partial}{\partial x}\log\theta(t,x), \tag{4.2}$$

$$\theta(t,x)=(4\pi\nu t)^{-1/2}\times\int_{-\infty}^{+\infty}dy\,\exp-\left(\frac{(x-y)^2}{4\nu t}+\frac{1}{2\nu}\int_0^y v_0(a)\,da\right). \tag{4.3}$$

Equation (4.3) is the solution of the heat equation

$$\frac{\partial\theta(t,x)}{\partial t}=\nu\frac{\partial^2\theta}{\partial x^2} \tag{4.4}$$

to which Burgers's equation is reduced by (4.2). $\theta(t,x)$ and $v(t,x)$ can be continued analytically both in the space and time variables (provided $\mathrm{Re}\,t>0$). However, to study the high-wave-number behavior at a given time there is no need to continue analytically in t. For fixed $t>0$, $\theta(t,z)$ is an entire function of the complex variable $z=x+i\xi$. Its logarithmic derivative $v(t,z)$ is a meromorphic function with poles at the zeros z_j of θ and residue -2ν (we discard multiple zeros which are nongeneric). This implies the following asymptotic expansion for the spatial Fourier transform $\hat{v}(t,k)$ for large positive k,

$$\hat{v}(t,k)\simeq -4i\pi\nu\sum_j{}^{\mathrm{up}}\,e^{ikz_j}. \tag{4.5}$$

We are thus led to study the properties of the zeros of the heat equation (4.4). The maximum principle for holomorphic functions implies that (i) $\theta(t,z)$ has no zeros for real z [use $\theta_0(x)>0$]; (ii) as time elapses new zeros of θ inside a bounded domain cannot appear without first crossing its boundary. Hence the zeros must either be generated at infinity or be present initially or both.[60]

Insight in the motion of singularities of Burgers's equation is provided by the polar representation.[61] Assume that at $t=0$,

$$v(z)=-2\nu\sum_j\frac{1}{z-z_j}. \tag{4.6}$$

Then this (polar) representation gives the exact solution of (4.1) at subsequent times if the poles move according to the equations of motion

$$\dot{z}_i=-2\nu\sum_{j\neq i}\frac{1}{z_i-z_j}. \tag{4.7}$$

Proof follows by substitution and use of the identity

$$\phi(x)\phi'(y)-\phi'(x)\phi(y)=\phi(x+y)[\phi'(y)-\phi'(x)], \tag{4.8}$$

which is satisfied by the function $\phi(x)=x^{-1}$ (Ref. 62).

The equations of motion of the poles have a structure very similar to the equations for the motion of vortices of equal strength K,

$$\dot{z}_i^*=-\frac{i}{2\pi}K\sum_{j\neq i}\frac{1}{z_i-z_j}. \tag{4.9}$$

Note, however, that (4.7) is always integrable whereas (4.9) is probably not when there are more than three vortices.[63] Observe also that two isolated vortices will rotate around each other but that two isolated poles will (eventually) move apart while aligning themselves parallel to the imaginary axis.

The high-Reynolds number limit

It is known that, in the limit $\nu\downarrow 0$, for prescribed initial conditions the solution of Burgers's equation develops shocks after a finite time. Evaluation of the integral in (4.3) by Laplace's method for $\nu\downarrow 0$ gives the position of the shocks. The presence of a small viscosity smoothes the shocks, thereby removing singularities from the real space domain. Indeed, consider a shock located at x_j with right and left limits of the velocity v_j^+ and v_j^-. The shock moves with the velocity $u_j=\frac{1}{2}(v_j^++v_j^-)$. The effect of a small viscosity is most easily obtained in the frame of reference moving with velocity u_j in which the shock is stationary, so that to leading order in ν one can drop the time derivative in (4.1). Integration of the resulting differential equation gives a hyperbolic tangent structure for the shock[57]

$$v(x)\simeq -\tfrac{1}{2}h_j\tanh[(x-x_j)h_j/4\nu), \tag{4.10}$$

where $h_j=v_j^--v_j^+$ is the shock strength. Analytic continuation of the tanh shows that $v(z)$ has pole singularities at

$$z_{j,n}=x_j+i\xi_{j,n}, \tag{4.11}$$

$$\xi_{j,n}=\pm\frac{4\nu}{h_j}\left(\frac{\pi}{2}+n\pi\right), \quad n=0,1,2,\ldots . \tag{4.12}$$

In the original reference frame a viscosity-smoothed shock may be viewed as a "parade" of equally spaced poles aligned parallel to the imaginary axis, the nearest being located $O(\nu)$ from the real axis.

Using (4.5) and (4.12) we obtain the asymptotic behavior of the spatial Fourier transform of the velocity ($k\to+\infty$)

$$\hat{v}(t,k)\simeq -4i\pi\nu\sum_j\sum_{n=0}^{\infty}e^{ikx_j}\exp\left[-\frac{4\nu k}{h_j}\left(\frac{\pi}{2}+n\pi\right)\right]. \tag{4.13}$$

Two regimes can be distinguished.

(i) An inertial range $k_0\ll k\ll H/\nu$, where k_0 and H are the inverse integral scale and the mean shock strength which are both $O(1)$ for times $O(1)$ but will eventually decay. In this range we sum the geometric series in (4.13) and expand the result for $\nu k/h_j\ll 1$; we thus obtain

$$\hat{v}(t,k)\simeq -ik^{-1}\sum_j h_j e^{ikx_j}. \tag{4.14}$$

(ii) A dissipation range $k\gg H/\nu$, in which only the $n=0$ singularity contributes to leading order, yielding

$$\hat{v}(t,k)\simeq -4i\pi\nu\sum_j e^{ikx_j}\exp(-2\nu\pi k/h_j). \tag{4.15}$$

The spectrum and the flatness

The spatial energy spectrum $E(t,k)$ and the flatness $F(t,k)$ of the spatially high-pass filtered solution of Burgers's equation can be calculated essentially the same way as for the NLL equation (cf. Sec. IIE) in terms of $N(t,h)$, the distribution of shockstrengths per unit length interval at time t. Leaving out purely numerical factors, the final results for the energy spectrum and the flataness are given below.

(i) Inertial range:

$$E(t,k)\sim\langle h^2\rangle k^{-2}, \quad F(t,K)\sim\frac{\langle h^4\rangle}{\langle h^2\rangle^2}K, \tag{4.16}$$

where

$$\langle h^n\rangle=\int_0^{\infty}h^nN(t,h)\,dh. \tag{4.17}$$

(ii) Dissipation range:

$$E(t,k)\sim\nu^2\int_0^{\infty}\exp(-4\nu\pi k/h)N(t,h)\,dh, \tag{4.18}$$

$$F(t,k)\sim\nu^{-1}\frac{\int_0^{\infty}h^3\exp(-8\nu\pi k/h)N(t,h)\,dh}{\left(\int_0^{\infty}h\exp(-4\nu\pi k/h)N(t,h)\,dh\right)^2}. \tag{4.19}$$

The inertial-range results are not new (see, for example, Ref. 64). Let us discuss now the dissipation-range results which require the knowledge of $N(t,h)$. There is a simple geometric construction to find the position and strength of all the shocks.[57] This has been used by Kida to give an integral representation of $N(t,h)$ valid for large times [Eq. (4.27) of Ref. 65]. His method can probably be extended to finite times and large shock strengths. We have not attempted to do this but we can still make some qualitative remarks. Since velocity is conserved along the motion, the shock strength can never exceed the largest velocity excursion $[\sup v_0(x)-\inf v_0(x)]$. We are thus led to distinguish two cases.

a. Bounded initial velocity distribution.

The shock distribution vanishes for $h>h_{\max}$ (which may depend on time). Let us assume for definiteness that, near $h_{\max}$, $N(t,h)$ behaves like $(h_{\max}-h)^{\alpha}$ ($\alpha>-1$); we then obtain

$$E(t,k)\sim k^{-(\alpha+1)}\exp(-8\nu\pi k/h_{\max}), \quad F(t,K)\sim K^{\alpha+1}. \tag{4.20}$$

b. Unbounded initial velocity distribution.

It seems very plausible that $N(t,h)$ will also be unbounded. For definiteness again we consider two examples.

(*b* 1). $N(t,h)\sim\exp(-h^{2\alpha})$, $h\to\infty$, $\alpha>0$. We obtain, omitting numerical and power-law prefactors (C_1 and C_2 are positive numerical constants)

$$E(t,k)\sim\exp[-C_1(\nu k)^{2\alpha/(2\alpha+1)}]$$
$$F(t,K)\sim\exp[C_2(\nu K)^{2\alpha/(2\alpha+1)}]. \tag{4.21}$$

(*b* 2) $N(t,h)\sim h^{-\alpha}$, $h\to\infty$. To ensure convergence of the integral in the numerator of the rhs of (4.19) we assume $\alpha>4$; we then obtain

$$E(t,k)\sim k^{-\alpha+1}, \quad F(t,K)\sim K^{\alpha}. \tag{4.22}$$

We see that all cases discussed above have unlimited intermittency and nonuniversal energy spectra (universality is here with respect to changes in the statistics of initial conditions). Note that for unbounded shock strengths the spectrum decreases more slowly than an exponential (it can even be algebraic). This is in disagreement with the results of closure calculations. The latter produce exponential energy spectra and no intermittency. This statement applies to the two-point closures known as Direct-Interaction, Lagrangian-History-Direct-Interaction, Test-Field-Model and Quasi-Normal-Markovian (eddy-

damped or viscosity-damped) discussed in Refs. 39–41 and 66 which become essentially identical in the dissipation range. Like for the NLL model (cf. Sec. II G), the exponential spectrum of closure is a consequence of the existence of a finite analyticity strip in complex position space.

Finally, a few comments on the use of Burgers's model with a random force f. By the Hopf-Cole transformation, Burgers's equation is then mapped into a heat equation with a potential, the solution of which is entire in the space variable when f is band limited (in space). Thus the velocity is again a meromorphic function. Most of the above analysis is unchanged but the determination of the shock-strength distribution may be more difficult. At finite Reynolds numbers it is conceivable that the "most-relevant" spatial singularities are triggered by occasional large excursions of the spatial gradient of the force (when allowed by the statistics) and can be obtained by a singular perturbation calculation.

V. SUMMARY AND DISCUSSION

Note that the more speculative questions relating to Navier-Stokes turbulence are discussed in Sec. VI.

A. NLL model and homogeneous turbulence

In Sec. II we have tested Kraichnan's[14] conjectures about intermittency in the dissipation range, using the NLL equations

$$m\dot{v} = -\gamma v - v^3 + f(t)\,, \tag{5.1}$$

with a band-limited random force $f(t)$ (the detailed specifications on the force (F1)–(F5) are listed in Sec. II A). We proved that for any m, $\gamma > 0$, the high-pass filtered solution $v_\Omega(t)$ has unlimited intermittency: its flatness tends to infinity with Ω. This results from the following mechanism. High-frequency behavior of the solution is controlled by the singularities of its analytic continuation $v(t+i\tau)$ to complex times (Sec. II B). A singularity at $z_* = t_* + i\tau_*$ ($\tau_* > 0$) produces a burst in the high-pass filtered solution, centered at t_* and with overall amplitude proportional to $e^{-\Omega\tau_*}$ (Sec. II C). For large Ω the dominant burst are produced by rare singularities with very small τ_* and are therefore well separated. We have shown that the singularities are branch points of exponent $-\frac{1}{2}$ (Sec. II B), the most relevant ones being located near the real zeros of $f(t)$ with a large slope $\dot{f}(t)$ (Sec. II D). In Sec. II E we have calculated the asymptotic expansion for high frequencies of the spectrum $E(\omega)$ and the flatness $F(\Omega)$. For a Gaussian force we have obtained

$$E(\omega) \simeq A_1 m^{5/4} \omega^{-7/12} \exp[-B_1(\omega m^{3/5})^{5/6}]\,, \tag{5.2}$$

$$F(\Omega) \simeq \mathfrak{A}_1 m^{-3/4} \Omega^{-1/4} \exp[+\mathfrak{B}_1(\Omega m^{3/5})^{5/6}]\,, \tag{5.3}$$

where A_1, B_1, $\mathfrak{A}_1$, and $\mathfrak{B}_1$ are positive numerical constants.[67]

We have shown that this high-frequency behavior is *not universal* with respect to the low-frequency forcing. A change in the statistics of the force cannot be absorbed in scaling factors. When the distribution of $w = |\dot{f}|$ (at times when $f = 0$) is of the form $\exp(-w^{2\alpha}/2)$, the exponent $\frac{5}{6}$ in (5.2) and (5.3) is changed to $5\alpha/(5\alpha+1)$. Nonuniversality comes about as follows. A singularity of exponent ρ at $z_* = t_* + i\tau_*$ produces a term $\omega^{-\rho-1} e^{i\omega t_*} e^{-\omega\tau_*}$ in the Fourier transform of the solution. Before averaging, the power-law prefactor is universal because the force does not affect the nature of the singularity (only the cubic and $\dot{v}$ terms are then relevant). The position, however, is not universal. When the amplitude factor $e^{-2\omega\tau_*}$ is averaged over the distribution of τ_*, slower than exponential decrease is obtained, which depends on the precise statistics of the force.

Our result contradicts usual ideas about homogeneous turbulence formulated for the first time by Kolmogorov[5] and discussed in detail, e.g., in Chap. VI of Ref. 3. According to such ideas (here reformulated in the time domain), the low-frequency forcing excites the high frequencies of the solution in a stepwise process; as ω increases, so does the number of steps, presumably leading to asymptotic independence and thus to universal statistical properties of the solution.

Further contact between the NLL model and homogeneous turbulence comes from the existence of an inertial range. When m and γ are both small there is a range of frequencies $[1 \ll |\omega| \ll \inf(m^{-3/5}, \gamma^{-3/2})]$ in which the force is zero and dissipative processes are negligible. In this range the spectrum follows an $\omega^{-8/3}$ law and the flatness increases as Ω^{+1} (Sec. II F). It appears that there is no energy-cascade argument, like in the Kolmogorov theory, from which the $\omega^{-8/3}$ spectrum (or any other power law) can be derived. This is so because the nonlinear term in the NLL equation has no associated conservation law. Note however, that, like in the Kolmogorov theory, the NLL inertial-range spectrum is universal. The reason is that this range is controlled by the real-time singularities that occur at infinite Reynolds number ($m = \gamma = 0$). Such singularities have again a universal exponent; being located in the real domain they produce, in the Fourier transform, universal power laws without exponential damping which are therefore unaffected by the averaging over the distribution of singularities.

Finally, we stress that, contrary to the existing semi-heuristic theories of homogeneous turbulence

which are often more conveniently formulated in Fourier space, it was essential for our systematic analysis of the NLL model to work in (complex) physical space.

B. Illusory asymptotic freedom

Classical nonlinear dynamical systems driven by random forces have a formal correspondence with nonlinear quantum fields which is discussed, e.g., in Refs. 10 and 42. It has been suggested that renormalized perturbation expansions can be useful for nonlinear classical systems, even when ordinary perturbation expansions are not appropriate. There are indeed cases where the renormalized coupling constant (depending on frequency ω or wave number k) tends asymptotically (i.e., for ω or k tending to zero or infinity) to zero (asymptotic freedom) or to some manageably small value. Examples have been found in the study of large-scale and long-time properties of critical dynamics[68] and randomly stirred fluids.[69-71] The low-frequency behavior of the NLL model can be similarly studied. We shall show now that this is generally not the case for its high-frequency behavior.

We begin with the case of a band-limited force, a condition which we shall later relax to discuss "illusory asymptotic freedom". We know that the high-frequency behavior is governed by the complex-time singularities of the analytic continuation of the velocity. Letting $z=t+i\tau$ approach a singularity z_*, we find that the ratio of the nonlinear term to the damping term

$$\frac{v^3(z)}{\gamma v(z)} \simeq \frac{m}{2\gamma(z-z_*)}, \tag{5.4}$$

tends to infinity. This, of course, is true irrespective of the strength of the nonlinear interaction on the real axis. A similar result holds in frequency space. Using the asymptotic expansion (2.46) we can evaluate the ratio of Fourier transforms of the cubic and damping terms; this gives a frequency-dependent coupling constant

$$g(\omega) \propto |\omega|, \tag{5.5}$$

which tends to infinity with ω. Observe that the following procedure would yield an incorrect result. We notice that $v^3/(\gamma v)=v^2/\gamma$, and use the Fourier transform of v^2/γ to estimate the coupling constant. This gives $\lim_{|\omega|\to\infty} g(\omega)=0$. The root of the discrepancy is that the latter procedure implicitly assumes that, in Fourier space, one can estimate integrals by factor counting procedures, e.g.,

$$\left| \int_{\omega_1+\omega_2+\omega_3=\omega} \hat{v}(\omega_1)\hat{v}(\omega_2)\hat{v}(\omega_3)\, d\omega_1\, d\omega_2 \right| \sim \omega^2 |\hat{v}(\omega)|^3 . \tag{5.6}$$

Equation (5.6) holds for (suitable) algebraic decrease, but not for exponential decrease. We stressed this rather obvious point because a similar misconception can lead to the conclusion that in the dissipation range of homogeneous turbulence the Reynolds number is very small.

The simplest renormalized perturbation approximation based on the field theoretic approach to classical nonlinear dynamics is the direct interaction approximation[24] (DIA). The investigation of Sec. II G shows that the DIA gives an incorrect description of the high-frequency behavior of the NLL model: We have obtained a universal exponential spectrum instead of a nonuniversal more slowly decreasing spectrum. This is a direct consequence of the growth of the coupling constant with frequency and will presumably not be cured by going to higher orders of renormalization.[72] An interesting observation is that for the case studied, the DIA is self-destructive because it has itself complex-time singularities and an indefinitely growing coupling constant as $\omega\to\infty$.

We now wish to discuss a case where the DIA and other renormalization procedures are wrong without being self-destructive. For this we take the NLL model with a Gaussian force but relax the assumption of band limitedness. With direct forcing of high frequencies nonlinear interactions are not needed to obtain a high-frequency response. It is then conceivable that ultraviolet asymptotic freedom will be obtained. This means that at high frequencies the nonlinear term is negligible (more precisely that its effect can be absorbed in a renormalization of the damping). In order to be able to use analytic-function techniques to investigate this question, we assume that the spectrum of the force is of the form ($\omega\to+\infty$)

$$\hat{\Phi}(\omega) \sim \omega^{\alpha} e^{-s\omega}, \quad s>0 . \tag{5.7}$$

The force $f(t)$ can then be extended analytically in the strip $|\mathrm{Im}z|<s/2$ at the edges of which it becomes singular. In the analyticity strip the force and its derivative, being Gaussian, can take arbitrary large values. Exactly as in the case of band-limited forces, singularities can occur arbitrarily close to the real axis. The results of Sec. II E are therefore unchanged. Obviously asymptotic freedom does not hold, however small the nonlinearity may be on the real axis. Let us see now what is predicted by perturbation theory for small nonlinearity. We introduce an expansion parameter g in front of the cubic term in the NLL

equation and assume that m and γ are $O(1)$. Expanding the spectrum in powers of g we obtain after standard manipulations ($\omega \to +\infty$)

$$E(\omega) \simeq C_1 \omega^{\alpha-2} e^{-s\omega} + g^2 C_2 \omega^{3\alpha-6} e^{-s\omega} + O(g^4), \quad (5.8)$$

where C_1 and C_2 are numerical factors depending on m and γ. When $\alpha < 2$, the g^2 term in (5.8) and also the higher-order terms are negligible compared to the g^0 contribution as $\omega \to \infty$. This suggests asymptotic freedom for $\alpha < 2$. The same conclusion is obtained from the DIA. Since the latter has a spurious branch of self-excited solutions (see Sec. II G), we must restrict ourselves to the branch reducing to the linear solution for $g = 0$. For this branch, when $\alpha < 2$, the singularity of the correlation function $U(z)$ closest to the real axis is the singularity of the correlation function of the force $\Phi(z)$ at $z_* = is$ [use Eq. (2.102′) and compare $6U^3(z)$ calculated from the linear solution with $\Phi(z)$ as $z \to z_*$]. Thus the DIA gives illusory asymptotic freedom, a result unlikely to be changed by higher orders of renormalized perturbations. The origin of the discrepancy may be understood by returning to the exact solution for the spectrum in the Gaussian case given in Sec. II E. The effect of the coupling constant g can be absorbed in a redefinition of v, m, and γ,

$$v = g^{-1/3}\tilde{v}, \quad m = g^{1/3}\tilde{m}, \quad \gamma = g^{1/3}\tilde{\gamma}. \quad (5.9)$$

Using this and (2.77) we see that the exact spectrum contains a factor $\exp(-B_1 \omega^{5/6} m^{1/2} g^{-1/6})$ with an essential singularity at zero coupling constant which is not captured by perturbation theory. This is a common situation in nonlinear field theory; see, e.g., Ref. 73.

We conclude that high-frequency intermittency is a problem of strong interactions dominated by singularities which, like many structures of nonlinear physics (solitons, shocks, instantons, vortices, dislocations, etc.) require nonperturbative techniques. It is only after explicit incorporation of such structures in the theory that the averaging by perturbative techniques becomes feasible.

C. Intermittency in nonlinear dynamics

Three examples of dynamical systems with high-frequency intermittency have been discussed in this paper; the NLL model (Sec. II), the Lorenz model (Sec. III) and Burgers's model (Sec. IV). A large class of dynamical systems should display such intermittency, in particular when the following conditions are fulfilled.

(i) The solutions tend to a statistical steady state which is truly random (nonvanishing fluctuations).

(ii) The solutions can be extended to complex times.

(iii) The solutions have singularities at random complex times.

(iv) The lower bound of the absolute value of the imaginary part of the singularities is not attained with a finite probability.

The above conditions are sufficient to apply the argument at the end of Sec. II C: The high-frequency filtered solution will consist of bursts which become increasingly sparse as the filter frequency $\Omega \to \infty$. Condition (i) requires that the system be either randomly driven (like the NLL model) or intrinsically stochastic. Condition (ii) is satisfied by any algebraic equation or ODE (or system of such equations) with holomorphic dependence on both the independent and dependent variables. This rules out for example the equation

$$m\dot{v} = -\gamma v - |v| v + f(t). \quad (5.10)$$

Condition (iii) can be fulfilled in two different ways. An extrinsic intermittency is obtained when the singularities of the solution just reflect the singularities of the force (e.g., the trivial case of a linear Langevin equation driven by an intermittent force). Intrinsic intermittency requires that the equation be nonlinear in the unknown.[74] Condition (iv) can be satisfied with a lower bound $\tau_{\min}$ which is zero (NLL model) or nonzero (Lorenz model).

We also note that intermittency is not restricted to the temporal domain as we have seen from the study of Burgers's equation (Sec. IV). In systems governed by partial differential equations with more than one space variable it becomes possible to consider multidimensional intermittency. This requires considerable mathematical machinery to extend the asymptotic theorem discussed in Sec. II C to functions of several complex variables.

Finally we stress that, even when we can demonstrate the existence of intermittency for a nonlinear equation, it may be difficult to calculate the high-frequency behavior. For this we need to know the nature of the complex-time singularities and their distribution (at least near $\tau_{\min}$). The method used to obtain the leading orders of the singularities of the NLL and Lorenz models can be applied to any nonlinear ODE with isolated singularities. One then just keeps the most relevant terms in the equation, i.e., those with the highest nonlinearity and the highest derivative. The perturbation method used in Sec. II D to locate the singularities of the NLL equation can be plausibly extended to other randomly driven systems. Observe that this expansion did not use an externally prescribed small parameter but was made possible by the existence of arbitrary large fluctuations in the derivative of the force. Extending

such ideas to intrinsically stochastic systems may require a better analytic understanding of strange attractors (in the real domain, to begin with).

VI. INTERMITTENCY AND NAVIER-STOKES TURBULENCE

We have demonstrated in this paper that the small-scale intermittency observed in turbulent flows is also present in much simpler models which can be handled by systematic techniques. Not enough is known about the properties of three-dimensional Navier-Stokes equation to allow us presently to proceed in a systematic way. In this final section, we shall be concerned with three questions.

(i) What is known about the analytic structure of the solutions of the Navier-Stokes equation? (By "known" we mean either rigorously proven or demonstrated by careful experiments or numerical simulations.)

(ii) Given this partial information and the results obtained on simpler dynamical systems, what can be conjectured concerning intermittency of Navier-Stokes turbulence?

(iii) What type of experiments and numerical simulations are relevant to the problem?

A. Analytic structure of the Navier-Stokes solutions

We shall not attempt to review what is known about existence, uniqueness, and regularity properties of the Navier-Stokes equation in three dimensions (initial-value problem). The reader will find a suitable presentation of such material in Chap. 5 of Ref. 41. Loosely expressed, such properties are known to hold (i) for arbitrary $t>0$ when the Reynolds number is "small"; (ii) for arbitrary viscosity and $0<t<T$ (T of the order of the initial eddy-turnover time) when the initial data are sufficiently differentiable; and (iii) for all times and viscosities in two space dimensions. Under the same condition it is possible to prove analyticity in the real space-time variables.[75] It must be stressed that, for $\nu>0$, the boundedness of v is sufficient to ensure this analyticity,[76] thereby allowing continuation to complex space times.

For large Reynolds numbers and large times there is no proof of the absence of real space-time singularities in three dimensions; there is, however, numerical evidence that it is so for Reynolds numbers up to four hundred (based on integral scale and rms velocity).[40] Furthermore, all existing experiments in turbulent flows at Reynolds numbers up to a million have produced a dissipation range suggesting that viscous dissipation is indeed capable of preventing real space-time singularities. Note, however, that it has been proven that such singularities, if they exist, are confined to a set of very small Hausdorff measure which may be easily missed both in simulations and experiments.[41,77]

B. Conjectures about Navier-Stokes turbulence

There is no analytic proof of the existence of real or complex domain singularities for the Navier-Stokes or the Euler equation ($\nu=0$). However, recently numerical evidence has been obtained that the three-dimensional Euler equation with a special choice of initial condition (the so-called Taylor-Green vortex) has a real singularity appearing at a finite time t_*; some information on the nature of this singularity has also been obtained.[78] Since the smoothing effect of viscosity is felt only in the real domain, we are led to conjecture that the solutions of the Navier-Stokes equation in three dimensions have singularities in the complex space-time domain, some of which become real as $\nu \downarrow 0$ (Ref. 79). We believe that for $\nu>0$ complex space singularities play a role in the backscattering of radio or acoustic waves with wavelength small compared to the dissipation scale. This may provide a tool for experimental investigation. There have been speculations that for $\nu \downarrow 0$ the real singularities are confined to a "fractal" set somewhat more space-filling than sheetlike structures.[12,13] If this is true, then for small ν the complex-time singularities at a fixed real point must come in clusters (possibly with a hierarchical structure); the number of singular points in the cluster increasing as ν decreases so that, in the limit, some Cantor-type set on the real-time axis obtains.

Whatever the precise nature of the singularities, we are led to conjecture that randomly driven flows at any Reynolds number have unlimited intermittency in the dissipation range and a nonuniversal energy spectrum depending on the statistics of the force. Gaining better understanding of the dissipation range could be important for numerical simulations with subgrid-scale modeling when it is desired to waste as little resolution as possible for the dissipation range without affecting larger scales.

In realistic high-Reynolds number turbulent flows driven, e.g., by prescribed shears or buoyancy forces, stochasticity will be at least in part of intrinsic nature. Like for the Lorenz model (Sec. III) the nature of the (possibly infinite dimensional) attractor that governs stochasticity determines the distribution of singularities. There is no need to be able to precisely characterize this attractor to conjecture that three-dimensional incompressible viscous flows, at any Reynolds number where they are turbulent, have also unlimited dissipation-range intermittency (more

precisely, an intermittency limited only by the breakdown of the hydrodynamic description and/or nonturbulent noise). We also expect that the dissipation range will have nonuniversal properties with respect to large-scale statistics. Experimentally determined dissipation-range spectra, when properly rescaled, appear to fall on a universal curve (see, e.g., Fig. 75 of Ref. 10); the measurements, however, are not very reliable. Indication that there may also be some lack of universality comes from measurements of (passive) temperature-derivative skewness. Nonzero values are obtained, suggesting small-scale anisotropies, possibly induced by large-scale features.[81]

The result of Sec. II F may suggest a reinterpretation of the inertial range of fully developed turbulence. When a turbulent flow is observed in the inertial range at a wave number $k<k_D$, the resolution $\sim k^{-1}$ is insufficient to distinguish between complex-space singularities, located within k_D^{-1} from real space, and real singularities of the Euler equation that may occur for $\nu \downarrow 0$. Such singularities are consistent with a universal power-law spectrum.

C. Suggestions for experiments and numerical simulations

Most existing experiments on the small scales of turbulence have focused on the measurement of statistical quantities relating either to the inertial range (e.g., power-law spectra and structure functions) or to the beginning of the dissipation range (e.g., dissipation-dissipation correlation function).[2,10,80,81] For such experiments it is important to have (at least) (i) very high Reynolds numbers; (ii) good stationarity; and (iii) reliable measurements down to scales somewhat less than the viscous cutoff. To test the conjecture on unlimited dissipation-range intermittency and also to obtain information on the singularities of the Navier-Stokes equation we must be able to probe much deeper into the dissipation range. This is difficult with the standard experimental setup because resolution is limited by probe size and the signal-to-noise ratio deteriorates. It seems advisable to relax condition (i) above: For a given geometric configuration a moderate Reynolds number experiment will have a bigger dissipation scale and thereby a bigger accessible dissipation range. Particularly low ratios of turbulent to nonturbulent noise can probably be achieved in liquid helium experiments (above the lambda transition).

Some care should be taken to keep the "turbulence level" (ratio of rms velocity fluctuations to mean velocity) as low as possible. Otherwise we might just observe "modulation intermittency" as now explained. According to the "Taylor hypothesis" the frequency ω of the time-recorded signal corresponds to the spatial wave number $k=|\omega|\overline{U}^{-1}$, where $\overline{U}$ is the mean flow velocity. A better approximation is $k=|\omega|U^{-1}$, where $U=\overline{U}+v$ is the instantaneous velocity which has approximately Gaussian fluctuations. Assume for a moment that the turbulence has no intermittency at all in its spatial structure (pure "Gedanken experiment"). Assume also that it has a faster than algebraic spatial spectrum, e.g., $\exp(-\eta k)$. Then the "instantaneous" temporal spectrum will be $\exp[-\eta|\omega|(\overline{U}+v)^{-1}]$. For

$$\frac{|\omega|}{\overline{U}/\eta}\ \frac{v_{\rm rms}}{\overline{U}} \gg 1 , \tag{6.1}$$

the exponential will tremendously amplify the fluctuation in v and thus produce high-frequency intermittency.[82] A possible way to distinguish, experimentally, between modulation and intrinsic spatial intermittency is to look for correlation between high-frequency bursts and negative peaks in the fluctuating velocity.

Experiments with a substantially accessible dissipation range can be used to give further support to the conjecture that there are complex-time singularities.[83] High-pass filtering of the velocity is the simplest technique for locating complex-time singularities [cf. Figs. 5(a) and 5(b)]. It must be pointed out that it is possible, although unlikely, that some high-frequency intermittent bursts are generated by mechanisms other than singularities such as modulation or transition[84] intermittency. More reliable quantitative information should be obtained by analytic continuation techniques. One conceivable method is to Fourier transform the sampled signal, suppress the very-high-frequency instrumental noise[85] and, then, use the temporal Fourier series continued directly to complex times. This Fourier series converges only in the strip $|\mathrm{Im}z|<\tau_{\rm min}$, where $\tau_{\rm min}$ is the imaginary part of the singularity closest to the real axis. The series, however, can also be used to calculate at various real times as many derivatives as reliable. It is then possible to use the Taylor expansion to locate singularities. Hopefully this method will yield information about the statistical distribution of singularities, their clustering properties, and their Reynolds number scaling properties.

It is likely that the singularities, say at a fixed real point as a function of complex time, have a universal nature as in the examples studied in this paper. It is therefore of interest to try to determine not just their positions but also their expon-

ent. This is very difficult. First, finding an exponent of divergence from a Taylor expansion may require considerably more accuracy than available. Second, even if accuracy problems can be overcome, it must be stressed that the apparent nature of the singularities may be changed by the geometry and the nonlinear response of the measuring device. For example, the finite length of a hot wire results in spatial integration; if we assume that the true velocity is meromorphic in the space and time variables, the measured signal will have logarithmic singularities at complex times which come in closely spaced pairs.

A possibly better way to obtain information on the nature of individual complex space-time singularities of the Navier-Stokes equation is to use numerical techniques. If the calculation is based on spectral methods the analytic continuation in space can be done by one of the methods described above. Since the nature of singularities is easily blurred by truncation, a very high spatial resolution is mandatory. For the analytic continuation in time it seems natural to use the Taylor expansion method. Simple initial conditions in two or three dimensions with just a few Fourier modes such as the Taylor-Green vortex[78] are advisable. Hopefully a combination of experimental and numerical techniques will tell us something about complex singularities which are, as we have seen in this paper, the atoms of small-scale viscous turbulent flow.

Note added in proof. Strong intermittency in the dissipation range (measured by the flatness of Fourier components) has been observed in direct numerical simulations of geostrophic turbulence by J. C. McWilliams and J. H. S. Chow (unpublished).

ACKNOWLEDGMENTS

We have benefited from discussions with C. Bardos, D. V. Chudnovsky, G. V. Chudnovsky, P. Coullet, J.-D. Fournier, J. Gollub, H. Greenside, B. I. Halperin, R. H. Kraichnan, M. Krook, C. E. Leith, P. C. Martin, J. Moser, D. R. Nelson, S. A. Orszag, J.-P. Poyet, H. A. Rose, P. Saffman, E. Siggia, J. Weiss, and K. G. Wilson. Particular thanks are due to Y. Gagne for providing us with unpublished data and for discussions. Numerical calculations were done at the Harvard Aiken Computer Laboratory and at the National Center for Atmospheric Research which is sponsored by the National Science Foundation, and at RCA-Laboratories, Zurich, where we have benefited from the kind assistance by G. K. Lang. The work was supported in part by a Vinton Hayes Fellowship Grant No. 1489, the National Science Foundation Grant No. DMR 77-10210, the Fonds National Suisse Grant No. 82.528.0.77, and the Kyburger Öpfelwähe Foundation Grant No. 294649. One of us (UF) would like to thank the National Center for Atmospheric Research and the RCA Laboratories of Zurich for their hospitality.

APPENDIX A: NUMERICAL SOLUTION IN THE REAL DOMAIN

1. Outline of difficulties connected with the high frequencies

Our goal is the accurate numerical calculation of the high-frequency behavior of solutions to the NLL equation (2.1)

$$m\dot{v} = -\gamma v - v^3 + f(t)\,, \tag{A1}$$

with periodic forcing, $f(t) = f(t+T)$. For the calculation of periodic solutions at first sight it would seem most natural to apply spectral methods[86] and solve the resulting nonlinear integral equation by iteration. Efficient calculation of the convolutions, however, involve Fast Fourier transform methods which require calculating the cubic term in t space on an equidistant grid. Since the high-frequency excitations are very localized in t space such an evenly spaced grid is, however, by no means optimal. Instead, a scheme in which the resolution (grid size) is locally adapted to the particular shape of the solution is more efficient but difficult to implement in a spectral method. These problems are circumvented if one works in t space with a method which permits variable step size. Owing to the faster than algebraic decrease of the Fourier amplitudes $\hat{v}(\omega)$ the determination of the high-frequency behavior makes high numerical precision mandatory.

In view of all these requirements, a method of integration based on the Taylor expansion of $v(t)$ is used which both facilitates the use of variable step size and permits the calculation of solutions whose accuracy is limited by round-off only. In Sec. A 2 we describe the solution of the initial-value problem by means of Taylor expansions. Section A 3 deals with a Newton method to satisfy periodic boundary condition. Section A 4 is devoted to the generation of band-limited Gaussian forces and Sec. A 5 describes the calculation of spectra.

2. Solution of initial-value problem by Taylor expansion

Suppose we know $v(t)$ for some real time t. Then using Eq. (A1) and its derivatives

$$v^{(n+1)}(t) = -\gamma v^{(n)}(t) - \sum_{i,j,k\geq 0;\, i+j+k=n} \frac{n!}{i!j!k!}\, v^{(i)}(t)v^{(j)}(t)v^{(k)}(t) + f^{(n)}(t)\,, \tag{A2}$$

we can recursively calculate any desired number of derivatives $v^{(n)}(t)$. It is then possible to calculate $v(t+\Delta)$ from the Taylor expansion

$$v(t+\Delta) = \sum_{n=0}^{M} \frac{\Delta^n}{n!}\, v^{(n)}(t) + R_M\,. \tag{A3}$$

The step size Δ is determined by either (i) the maximum frequency $\Omega_{\max}$ for which we want to calculate the Fourier amplitudes $\hat{v}(\omega)$, or (ii) the radius of convergence of the Taylor series which is determined by the distance of the nearest singularity (cf. Sec. II B). The remainder term R_M can then be made smaller than the round-off error by taking a sufficiently large number M of derivatives. Making repeated use of (A2) and (A3) we can calculate $v(t)$ for arbitrary real t from the initial condition $v(t_0) = v_0$.

3. Newton's method for periodic solutions

In order to obtain periodic solutions to Eq. (A1) we use an iterative method. For this purpose we study the mapping ϕ: $v(0) \to v(T)$ (cf. Sec. II A). The desired initial value v^*, satisfying the periodic boundary condition

$$v^* = \phi(v^*)\,, \tag{A4}$$

is the unique fixed point of this map. We determine v^* by means of a Newton iteration to calculate the zero of the function $\phi(v) - v$. Derivatives $d\phi/dv$ are approximated by finite difference expressions. Table II shows the convergence of this iteration for the solution of Eq. (A1) with $m = 1$, $\gamma = 0$, and $f(t) = \cos t + 2\cos 2t$. For the integration, a step size $\Delta = \frac{2}{64}\pi$ and a maximum of 40 derivatives is used. For the example displayed in Fig. 4 [Gaussian force with 10 modes, $\gamma = 0.1$, and $m = (0.3)^{1/2}$], two iterations are required to satisfy the periodic boundary condition with 14 digit accuracy.

4. Generation of band-limited Gaussian forces

The periodic force $f(t)$ is defined by its Fourier representation Eq. (2.3)

$$f(t) = \sum_{|\omega_n| \leq B} e^{-i\omega_n t} \hat{f}_n\,, \quad \omega_n = \frac{2\pi n}{T}\,. \tag{A5}$$

Writing the Fourier component $\hat{f}_n$ in terms of its modulus a_n and phase ϕ_n and utilizing the Hermitian symmetry $\hat{f}_{-n} = \hat{f}_n^*$ we rewrite $f(t)$ as

$$f(t) = a_0 + 2\sum_{n=1}^{N_M - 1} a_n \cos(\omega_n t - \phi_n)\,. \tag{A6}$$

TABLE II. Convergence of Newton iteration for the calculation of periodic solutions to the NLL.

Iteration	$x(0)$	$x(2\pi)$
1	1	0.905 380 069 283 83
2	0.905 380 069 283 83	0.905 379 178 927 00
3	0.905 379 178 927 00	0.905 379 178 917 95
4	0.905 379 178 917 94	0.905 379 178 917 94

The coefficients a_i are independent Gaussian-distributed random variables while the phases ϕ_n are independent random variables uniformly distributed in the interval $[0, 2\pi[$. Throughout this paper numerical calculations with Gaussian forces are done with a flat spectrum, i.e., $\langle a_i^2\rangle \equiv \langle a_0^2\rangle$, $i = 1, \ldots, N_M - 1$, where N_M is the number of modes. The condition $\langle f^2\rangle = 1$ implies a variance

$$\langle a_i^2\rangle = \frac{1}{2N_M - 1}\,, \tag{A7}$$

while the condition $\langle \dot{f}^2\rangle = 1$ requires a period

$$T = 2\pi\left(\frac{N_M(N_M-1)}{3}\right)^{1/2} \tag{A8}$$

and a bandwidth $B = (N_M - 1)2\pi/T$,

$$B = \sqrt{3}\left(\frac{N_M - 1}{N_M}\right)^{1/2}. \tag{A9}$$

For the generation of uniformly distributed pseudo-random numbers the usual power-residue method is employed. The generation of Gaussian distributed pseudo-random numbers with unit variance is done by the standard procedure of adding 12 pseudo-random numbers with uniform distribution in the interval $[-\frac{1}{2}, \frac{1}{2}[$.

5. Calculation of spectra

The spectra shown in Sec. II F are obtained by averaging $|\hat{v}(\omega)|^2$ over 20 realizations of the Gaussian force. Denoting by $\hat{v}_i(\omega)$ the Fourier components of the solution for the ith realization of the force, we define

$$\bar{E}_n = \frac{1}{N_R}\sum_{i=1}^{N_R} |\hat{v}_i(\omega_n)|^2\,, \tag{A10}$$

where N_R is the number of realizations. In addition, averaging over five adjacent frequencies is used to obtain a more rapid convergence

$$E_n = \frac{1}{5}\sum_{k=n-2}^{n+2} \bar{E}_k\,. \tag{A11}$$

All these calculations are done using for the integration a step length $\Delta = T/2048$. The Fourier amplitudes $\hat{v}(\omega)$ are calculated for $|\omega| \leq 1024 \times 2\pi/T$.

APPENDIX B: NUMERICAL INTEGRATION IN THE COMPLEX DOMAIN

1. Analytic continuation by Taylor expansion

While the effective damping $\gamma_{\text{eff}}(t)=\gamma+v^2(t)$ is positive on the real t axis and therefore assures stable numerical integration in the direction of increasing time, integration in the complex domain suffers from the same type of instability problems as are encountered in integration in the negative time direction. This difficulty can be circumvented by a combination of (i) high-precision arithmetic, and (ii) a stable numerical method minimizing the effects of round-off errors, by using as large integration steps as the analytic structure of the solution $v(t)$ permits. This requires the use of a high-order numerical scheme.

The method of Taylor series expansion of $v(t)$, outlined in Appendix A, fulfills these requirements. In the present work we employ up to 100 derivatives.[87] It then turns out to be possible to perform the analytic continuation using single precision (seven digit) arithmetic and still obtain accurate information about the analytic structure of $v(t)$.

2. Locating singularities

As discussed in Sec. II B the ratios of subsequent derivatives $v^{(n)}(t)$ can be used to calculate the position of the nearest singularity. Assuming that the radius of convergence of the Taylor series at the point z is determined by a single singularity on the circle of convergence, the sequence

$$z_n^*(z)=z+(n-\tfrac{1}{2})\frac{v^{(n-1)}(z)}{v^{(n)}(z)} \tag{B1}$$

converges, as $n\to\infty$, to the position z_* of the singularity nearest to z [cf. Eq. (2.30)]. Since the singularities of $v(z)$ occur in complex conjugate pairs, Eq. (B1) can only be used if derivatives $v^{(n)}(z)$ are calculated on a point not lying on the real-time axis.

In Table III we list $z_n^*(z)$ for the four singularities of $v(t)$ corresponding to the choice

$$f(t)=\cos t+2\cos 2t,\quad m=1,\quad \gamma=0, \tag{B2}$$

and periodic solution.

This is obtained as follows.

(i) We solve Eq. (A1) for the periodic solution on the real t axis. We obtain $v(0)=0.905\,379$ (cf. Table II).

(ii) We integrate along the imaginary axis from 0 to $Z_i=0.45i$. This leads to $v(Z_i)=2.965\,694+i\ 1.754\,915$.

(iii) Integrating from Z_i to $Z_f=Z_i+2\pi$ we obtain information about all four singularities in the upper half of the complex time plane.

TABLE III. Locating singularities by numerical analytic continuation using ratios of nth-order derivatives.

Rez	Imz	n	Re$z_n^*(z)$	Im$z_n^*(z)$
0	0.45	41	−0.018 758	0.487 572
		46	−0.018 758	0.487 572
0.122 718 47	0.45	17	−0.018 758	0.487 572
		23	−0.018 758	0.487 572
0.220 893 26	0.45	17	−0.018 759	0.487 572
		23	−0.018 758	0.487 572
1.300 816 10	0.45	20	1.913 695	0.611 510
		25	1.913 697	0.611 510
1.988 039 50	0.45	26	1.913 699	0.611 510
		31	1.913 699	0.611 510
3.411 573 90	0.45	29	3.515 108	0.938 118
		34	3.515 107	0.938 118
3.607 923 50	0.45	33	3.515 106	0.938 118
		38	3.515 106	0.938 118
4.491 496 10	0.45	43	4.504 307	0.625 037
		48	4.504 307	0.625 037
4.835 108 80	0.45	15	4.504 315	0.625 047
		20	4.504 308	0.625 039
6.258 644 10	0.45	49	6.264 426	0.487 572
		54	6.264 426	0.487 572

Inspection of Table III shows that the sequences $Z_n^*(t)$ allow a very accurate determination of Z_*. In particular, as long as Z_* is the singularity nearest to Z, varying Z leads to extrapolated values of Z_* which are independent of Z.

3. Integration around singularities

The calculation of analytic continuations along contours surrounding singularities represents a severe test for the numerical precision. The method based on the Taylor expansion of $v(t)$ outlined in Appendix A 1 handles this problem without difficulty.

In Table IV we present results obtained by integration around the singularity at $Z_*=6.264\,426+0.487\,572\,i$ for the example $f(t)=\cos t+2\cos 2t$, $m=1$, $\gamma=0$ (cf. Table III). Integration is done along the contours

$$C_1:\ 2\pi\to\tfrac{15}{8}\pi+0.6i\to 2\pi+0.6i\to 2\pi$$
$$\to\tfrac{15}{8}\pi\to 2\pi+0.8i\to 2\pi,$$
$$C_2:\ 2\pi\to\tfrac{17}{8}\pi+0.7i\to\tfrac{15}{8}\pi+0.7i\to 2\pi$$
$$\to\tfrac{17}{8}\pi+0.55i\to\tfrac{15}{8}\pi+0.6i\to 2\pi.$$

As can be seen from Table IV, turning around the singularity twice reproduces the starting value with six digit accuracy. Note that turning around the singularity once leads to complex values of $v(t)$ on the real t axis. The calculation is done using seven digit arithmetic. A maximum number of 50 derivatives is used.

TABLE IV. Numerical integration around the singularity at $Z=6.264\,426+i0.487\,572$. Turning around the singularity once leads to complex values on the real-time axis. Turning around the singularity twice reproduces the starting values with great precision.

	Rez	Imz	ReV	ImV
Contour 1	2π	0	0.905 379	0
	$\frac{15}{8}\pi$	0.6	−0.795 078	1.182 031
	2π	0.6	−1.571 905	1.557 923
	2π	0	−0.790 033	−1.217 905
	$\frac{15}{8}\pi$	0	−0.661 443	−1.245 363
	2π	0.8	1.080 353	−0.075 323
	2π	0	0.905 382	0.000 001
Contour 2	2π	0	0.905 379	0
	$\frac{17}{8}\pi$	0.7	1.701 895	−0.280 696
	$\frac{15}{8}\pi$	0.7	−0.660 318	−1.220 406
	2π	0	−0.790 033	−1.217 905
	$\frac{17}{8}\pi$	0.55	−0.242 588	−0.094 697
	$\frac{15}{8}\pi$	0.6	−0.795 079	1.182 031
	2π	0	0.905 380	0.000 003

APPENDIX C: THE INNER ASYMPTOTIC EQUATION

We study the differential equation

$$\frac{dx}{d\zeta}=-x^3+\zeta\,,\quad \zeta=\xi+i\eta\,, \tag{C1}$$

in the real and complex domains. The boundary conditions are given at real infinities

$$x(\xi)\simeq\xi^{1/3},\quad \text{for } \xi\to\pm\infty\,, \tag{C2}$$

where the cubic root is understood to have the same sign as ξ. For large $|\zeta|$, Eq. (C1) has an asymptotic series solution

$$x(\zeta)=\zeta^{1/3}[1-\tfrac{1}{9}\zeta^{-5/3}+O(\zeta^{-10/3})]\,. \tag{C3}$$

The determination that satisfies the $+\infty$ boundary condition (C2), if followed along a great half circle in the upper or lower half-plane, will not satisfy the $-\infty$ boundary condition. Therefore, the solution of (C1) with the boundary condition (C2), if it exists, must have at least a singularity at finite distance. By a standard argument (Sec. IIB), singularities have exponent $-\frac{1}{2}$. Singularities for finite real times are ruled out. Indeed, the nonlinear term in Eq. (C1) is dissipative; therefore, if x is finite for some ξ it will be finite for all $\xi'>\xi$.

To demonstrate uniqueness of the solution, let us tentatively assume the existence of two solutions x and y such that for some ξ_2,

$$x(\xi_2)-y(\xi_2)\neq 0\,. \tag{C4}$$

The difference $z=x-y$ satisfies

$$\frac{dz}{d\xi}=-z(x^2+xy+y^2)=-z\mu\,. \tag{C5}$$

Notice that for $\xi\to\pm\infty$,

$$\mu(\xi)\simeq 3\xi^{2/3}\,. \tag{C6}$$

From (C5) we have

$$z(\xi_1)=z(\xi_2)\exp\left(-\int_{\xi_2}^{\xi_1}\mu(\xi)\,d\xi\right). \tag{C7}$$

Then, letting $\xi_1\to-\infty$ and using (C6), we find that

$$z(\xi_1)\simeq z(\xi_2)\exp(-\tfrac{9}{5}\xi_1^{5/3})\,, \tag{C8}$$

which is not consistent with the $-\infty$ boundary condition.

We have not been able to prove the existence of a solution but we can demonstrate existence numerically. We use the Taylor expansion method described in Appendix A. The integration is started at large negative times using a value of x given by the first two terms of the asymptotic expansion (C3). This way the solution can be calculated in the range $t=-20$ to $t=+20$ with an accuracy of 10^{-12} near to $t=0$. The resulting graph is plotted in Fig. 8. Perfect match with the $+\infty$ boundary condition is obtained.

Analytic continuation to complex ζ is done by the complex Taylor expansion method of Appendix B. On the physical sheet (analytic continuation by the shortest path from the real axis) we have found two pairs of complex conjugate singularities with exponent $\rho=-\frac{1}{2}$, located at

$$\zeta_*=\xi_*+i\eta_*\simeq 1.707\,907+i\ 0.778\,600 \tag{C9}$$

and

$$\zeta_{**}=\xi_{**}+i\eta_{**}\simeq 2.198\,79+i\ 1.869\,63 \tag{C10}$$

and at the complex conjugate positions. We have not found further singularities on the physical sheet.

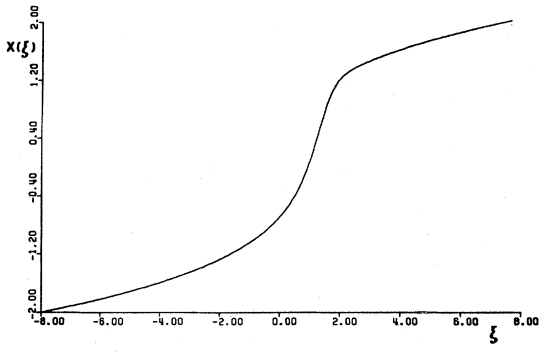

FIG. 8. The solution of Eq. (2.60), $dx/d\xi=-x^3+\xi$, with $x\sim\xi^{1/3}$ for large $|\xi|$.

*Present address.

[1]G. K. Batchelor, Proc. R. Soc. London, Ser. A 190, 238 (1949).

[2]Y. Gagne, thesis, Institut de Mécanique de Grenoble, France, 1980 (unpublished). The experiment of Gagne uses a grid-generated turbulent flow in a rectangular channel. The mean velocity $\overline{U}=10.5$ m/s; rms fluctuation is 0.07 $\overline{U}$. Reynolds number based on Taylor scale is $R_\lambda=230$. The longitudinal velocity component is measured with a hot wire (diameter 1 μm, length 0.3 mm). The frequency corresponding to the Kolmogorov dissipation scale is $f_*=8.3$ kHz. Signal is sampled at 38.4 kHz. The intermittent bursts shown in Fig. 1 are obtained with a digital band-pass convolution filter centered at $f_M=14.5$ kHz (width $\Delta f/f=0.28$). Signal-to-noise ratio at f_M is 3.

[3]G. K. Batchelor, *The Theory of Homogeneous Turbulence* (Cambridge University Press, Cambridge, England, 1960).

[4]A. Y. Kuo and S. Corrsin, J. Fluid Mech. 50, 285 (1971).

[5]A. N. Kolmogorov, C. R. (Dokl.) Acad. Sci. URSS 30, 301 (1941).

[6]E. D. Siggia and G. S. Patterson, J. Fluid Mech. 86, 567 (1978).

[7]S. A. Orszag and C.-M. Tang, J. Fluid Mech. 90, 129 (1979).

[8]E. D. Siggia (unpublished).

[9]L. D. Landau and E. M. Lifshitz, *Fluid Mechanics* (Pergamon, New York, 1963).

[10]A. S. Monin and A. M. Yaglom, *Statistical Fluid Mechanics: Mechanics of Turbulence*, edited by J. L. Lumley (MIT Press, Cambridge, Mass., 1975), Vol. 2; updated and augmented edition of Russian original, *Statisicheskaya Gidromekhanika* (Nauka, Moscow, 1965).

[11]R. H. Kraichnan, J. Fluid Mech. 62, 305 (1974).

[12]B. B. Mandelbrot, in *Turbulence and Navier-Stokes Equation*, edited by R. Temam, Vol. 565 of Lecture Notes in Mathematics (Springer, Berlin, 1976), p. 121.

[13]U. Frisch, P.-L. Sulem, and M. Nelkin, J. Fluid Mech. 87, 719 (1978).

[14]R. H. Kraichnan, Phys. Fluids 10, 2080 (1967).

[15]The random force overrules the possibility that the flow can be intrinsically stochastic (see Sec. III).

[16]U. Frisch, M. Lesieur, and A. Brissaud, J. Fluid Mech. 65, 145 (1974).

[17]W. Heisenberg, Z. Phys. 124, 628 (1948).

[18]H. L. Grant, R. W. Stewart, and A. Moilliet, J. Fluid Mech. 12, 241 (1962).

[19]When the high-frequency excitation decreases sufficiently fast with frequency, as is the case in all the problems considered in this paper, there is no essential difference between high-pass and band-pass filtering, provided the bandwidth is large compared to the inverse correlation time.

[20]U. Deker and F. Haake, Phys. Rev. A 12, 1629 (1975).

[21]H. King, U. Deker, and F. Haake, Z. Phys. B 36, 205 (1979).

[22]C. Bender, F. Cooper, G. Guralnik, H. Rose, and D. Sharp, J. Stat. Phys. (in press).

[23]K. Ziegler and H. Horner, Z. Phys. B (in press).

[24]R. H. Kraichnan, J. Fluid Mech. 5, 497 (1959).

[25]E. N. Lorenz, J. Atmos. Sci. 20, 130 (1963).

[26]J. M. Burgers, *The Nonlinear Diffusion Equation* (D. Reidel, Boston, 1974).

[27]By changes of independent and dependent variables it is possible to reduce the NLL equation to a form with zero damping. However, the transformed force will not be stationary.

[28]We do not explicitly display a realization variable; ω in this paper is always a real frequency.

[29]R. K. Otnes and L. Enochson, *Digital Time Series Analysis* (Wiley, New York, 1972).

[30]E. Hille, *Ordinary Differential Equations in the Complex Domain* (Wiley, New York, 1976).

[31]H. T. Davis, *Introduction to Nonlinear Differential and Integral Equations* (Dover, New York, 1962).

[32]R. Courant and D. Hilbert, *Methods of Mathematical Physics* (Interscience, New York, 1962).

[33]The convergence radius $r(t)$ is a random function which, as we shall see in Sec. II D, can take arbitrary small positive values.

[34]H. Cartan, *Théorie Elémentaire des Fonctions Analytiques d'Une ou Plusieurs Variables Complexes* (Hermann, Paris, 1961).

[35]G. F. Carrier, M. Krook, and C. E. Pearson, *Functions of a Complex Variable* (McGraw-Hill, New York, 1966).

[36]A. B. Migdal and V. Krainov, *Approximation Methods in Quantum Mechanics* (Benjamin, New York, 1969).

[37]For the algebraic case ($m=0$) the distribution of singularities can be calculated using (2.40).

[38]R. H. Kraichnan, *Proceedings of Symposium in Applied Mathematics* (Amer. Math. Soc., 1962), Vol. 13, p. 199.

[39]D. C. Leslie, *Developments in the Theory of Turbulence* (Clarendon, Oxford, 1973).

[40]S. A. Orszag, in *Fluid Dynamics*, Lectures of the Les Houches Summer School, edited by R. Balian and J. L. Peube (Gordon and Breach, New York, 1977), p. 235.

[41]H. A. Rose and P.-L. Sulem, J. Phys. (Paris) 39, 441 (1978).

[42]P. C. Martin, E. D. Siggia, and H. A. Rose, Phys. Rev. A 8, 423 (1973).

[43]R. H. Kraichnan, J. Math. Phys. (N.Y.) 2, 124 (1961); 3, 205(E) (1962).

[44]M. Lesieur, U. Frisch, and A. Brissaud, Ann. Geophys. (Paris) 27, 151 (1971).

[45]R. H. Kraichnan, J. Math. Phys. (N.Y.) 3, 496 (1962).

[46]A possible way to eliminate this difficulty, communicated by H. Rose, is to change the NLL equation into a quadratic system by introducing an additional field, for example $X(t)=v^2(t)$. A comparison of various field-theoretic procedures from the viewpoint of realizability has been made by S. Gauthier, M.-E. Brachet, and J.-D. Fournier (unpublished).

[47]When the Reynolds number is small, DIA and exact solution agree over a wide frequency range.

[48]G. A. Kuzmin (unpublished).

[49]D. Ruelle and F. Takens, Commun. Math. Phys. 20, 167 (1971); 23, 343 (E) (1971).

[50]D. Ruelle, Phys. Lett. 72A, 81 (1979).

[51]D. Ruelle, in *Turbulence and Navier-Stokes Equation*, edited by R. Temam, Vol. 565 of Lecture Notes in Mathematics (Springer, Berlin, 1976), p. 146.

[52]P. Manneville and Y. Pomeau, Phys. Lett. 75A, 1 (1979).

[53]C. Tresser, P. Coullet, and A. Arneodo, J. Phys. (Paris) Lett. 41, L-243 (1980).

[54]J. P. Gollub and S. V. Benson, J. Fluid Mech. 100, 449 (1980); J. Maurer and A. Libchaber, J. Phys. (Paris)

Lett. 40, L-419 (1979).
[55]This was conjectured by J. Léorat, A. Pouquet, and U. Frisch, J. Fluid Mech. (in press) and has been observed in direct numerical simulations of the MHD equations by M. Meneguzzi, A. Pouquet, and U. Frisch (unpublished). A similar phenomenon has been observed in a five mode system by E. Spiegel, Ann. N. Y. Acad. Sci. (in press).
[56]M. Tabor and J. Weiss (unpublished).
[57]H. Segur, Lecture Notes Enrico Fermi School of Physics, Varenna, Italy (1980) (unpublished).
[58]K. A. Robbins, SIAM (Soc. Ind. Appl. Math.) J. Appl. Math. 36, 457 (1979).
[59]E. Hopf, Commun. Pure Appl. Mech. 3, 201 (1950); J. D. Cole, Q. Appl. Math. 9, 225 (1951).
[60]Examples can be constructed of initial conditions $v_0(z)$ with no singularity (e.g., $e^{-\lambda \cos z}$ with large positive λ) such that $v(t,z)$ has pole singularities at subsequent times. We do not know if this is generic behavior.
[61]F. Calogero, Lett. Nuovo Cimento 13, 411 (1975); D. V. Chudnovsky and G. V. Chudnovsky, Nuovo Cimento 40B, 339 (1977).
[62]The polar representation seems to have been discovered in connection with the Korteweg-de Vries equation: M. D. Kruskal, in *Nonlinear Wave Motion*, edited by A. Newell (American Mathematical Society, Providence, 1974), p. 61; J. Moser, Adv. Math. 16, 197 (1975). It is now known to be intimately connected with the integrability of systems of finitely or infinitely many particles interacting via the potential $G\wp(x)$ where $\wp$ is the Weierstrass elliptic function. This is discussed in Refs. 61 and also in D. V. Chudnovsky, Lett. Nuovo Cimento 23, 503 (1978); D. V. Chudnovsky, J. Math. Phys. 20, 2416 (1979).
[63]H. Aref and N. Pomphrey, Phys. Lett. 78A, 297 (1980).
[64]P. G. Saffman, in *Topics in Nonlinear Physics*, edited by N. J. Zabusky (Springer, Berlin, 1968), p. 485.
[65]S. Kida, J. Fluid Mech. 93, 337 (1979).
[66]T. Tatsumi, S. Kida, and J. Mizushima, J. Fluid Mech. 85, 97 (1978); U. Frisch, M. Lesieur, and D. Schertzer, J. Fluid Mech. 97, 181 (1980).
[67]In the example considered at the end of Ref. 14, intermittency is produced by a multiplicative process with no underlying singularities; this explains the much slower algebraic growth of the flatness.
[68]B. I. Halperin, P. C. Hohenberg, and E. D. Siggia, Phys. Rev. B 13, 1299 (1976).
[69]D. Forster, D. R. Nelson, and M. J. Stephen, Phys. Rev. A 16, 732 (1977).
[70]J.-D. Fournier and U. Frisch, Phys. Rev. A 17, 747 (1978).
[71]C. De Dominicis and P. C. Martin, Phys. Rev. A 19, 419 (1979).
[72]With Navier-Stokes turbulence, the DIA has an additional difficulty because it violates Galilean invariance; however, as pointed out in Ref. 48, this is of no concern in the far dissipation range where the viscous decay time is much shorter than the advection time by the energy-carrying eddies.
[73]C. M. Bender and T. T. Wu, Phys. Rev. 184, 1231 (1969).
[74]Squaring a Gaussian random function as in the experiment of D. A. Kennedy and S. Corrsin, J. Fluid Mech. 10, 366 (1961) is not going to produce complex-time singularities. This explains why no intermittency was found. However, applying a (band-limited) voltage across a nonlinear resistor (e.g., $R=R_0+\beta I^2$) should produce an intermittent current $I(t)$.
[75]C. Bardos and S. Benachour, An. Sc. Norm. Sup. Pisa, Serie IV, 4, 468 (1977).
[76]S. Kaniel and M. Shinbrot, Arch. Rat. Mech. Analys. 24, 302 (1967), have shown that uniform boundedness in space and time of the velocity (and even weaker conditions) implies boundedness of first and second spatial derivatives. Analyticity follows then, using an argument of T. Kato and M. Fujita, Rend. Semin. Mat. Univ. Padova 32, 243 (1962).
[77]V. Scheffer, C. R. Acad. Sci. 282, A 121 (1976); Pac. J. Math. 66, 535 (1976).
[78]R. H. Morf, S. A. Orszag, and U. Frisch, Phys. Rev. Lett. 44, 572 (1980).
[79]In two dimensions real singularities are possible only if present initially (e.g., Helmholtz vortices). This follows from a regularity theorem for the Euler equation with smooth initial conditions proved by W. Wolibner, Math. Z. 37, 668 (1933); see also Ref. 41. This theorem does not rule out complex singularities.
[80]P. G. Mestayer, C. H. Gibson, M. F. Coantic, and A. S. Patel, Phys. Fluids 19, 1279 (1976); R. A. Antonia and C. W. Van Atta, J. Fluid Mech. 84, 561 (1978); J. Atmos. Sci. 36, 99 (1979); Phys. Fluids 22, 2430 (1979).
[81]C. W. Van Atta and W. Y. Chen, J. Fluid Mech. 44, 145 (1970); F. H. Champagne, J. Fluid Mech. 86, 67 (1978).
[82]This is essentially the same as Kraichnan's (see Ref. 14) argument discussed in Sec. I B. Observe that there are no complex-time singularities underlying modulation intermittency.
[83]Singularities of the three-dimensional Navier-Stokes equation, if they exist, are located on some manifold of the complex space time C^4 which, probably, does not intersect the real domain R^4. For a given real point in R^3 there will in general be complex-time singularities and vice versa.
[84]Y. Pomeau and P. Manneville, in *Intrinsic Stochasticity in Plasmas* edited by G. Laval and D. Grésillon (Editions de Physique, Orsay, France, 1979), p. 329.
[85]The instrumental noise has typically an algebraic spectrum and thereby prevents analytic continuation to complex times.
[86]D. Gottlieb and S. A. Orszag, *Numerical Analysis of Spectral Methods: Theory and Applications* (Soc. Industr. Appl. Math., Philadelphia, 1977).
[87]A very sensitive test of the numerical integration was carried out using the exactly solvable example with $f(t)=\cos t+\cos^3 t-\sin t$, $v(0)=\gamma=m=1$, whose solution is $v(t)=\cos t$. Starting at $t=0$ and integrating along the imaginary axis the solution obtained using the fourth-order Runge-Kutta scheme becomes unstable (leading to overflow) at $z=2.6i$, $2.9i$, and $3.13i$ for step lengths $\Delta t=0.03$, 0.015, and 0.01, respectively. The Taylor method, on the other hand, remains stable, giving results accurate to six digits at $z=3.25i$ for a step length $\Delta t=0.02$ and a maximum of 80 derivatives. Single precision (seven digit) arithmetic was used.